

UNDERSTANDING THE BEHAVIOUR OF MODERN REINFORCED
CONCRETE BEAM-COLUMN JOINTS TOWARDS THE DEVELOPMENT OF
A SIMPLIFIED STRUCTURAL MODEL

A THESIS SUBMITTED TO
THE BOARD OF GRADUATE PROGRAMS
OF
MIDDLE EAST TECHNICAL UNIVERSITY, NORTHERN CYPRUS CAMPUS

BY

ORHAN SAHUTOGLU

IN PARTIAL FULFILLMENT OF THE REQUIREMENTS
FOR
THE DEGREE OF MASTER OF SCIENCE
IN SUSTAINABLE ENVIRONMENT AND ENERGY SYSTEMS PROGRAM

JULY 2022

Approval of the Board of Graduate Programs

Prof. Dr. Cumali Sabah
Chairperson

I certify that this thesis satisfies all the requirements as a thesis for the degree of Master of Science

Assoc. Prof. Dr. Ceren İnce
Derogar
Program Coordinator

This is to certify that we have read this thesis and that in our opinion it is fully adequate, in scope and quality, as a thesis for the degree of Master of Science.

Asst. Prof. Dr. Ali Şahin Taşlıgedik
Supervisor

Examining Committee Members

Assoc. Prof. Dr. Volkan Esat	METU NCC/Mechanical Engineering	_____
Asst. Prof. Dr. Ali Şahin Taşlıgedik	METU NCC/Civil Engineering	_____
Asst. Prof. Dr. İsmail Safkan	EUL/Civil Engineering	_____

I hereby declare that all information in this document has been obtained and presented in accordance with academic rules and ethical conduct. I also declare that, as required by these rules and conduct, I have fully cited and referenced all material and results that are not original to this work.

Name, Last name : Orhan Sahutoglu

Signature :

ABSTRACT

UNDERSTANDING THE BEHAVIOUR OF MODERN REINFORCED CONCRETE BEAM-COLUMN JOINTS TOWARDS THE DEVELOPMENT OF A SIMPLIFIED STRUCTURAL MODEL

Şahutoğlu, Orhan

Master of Science, Sustainable Environment and Energy Systems Program

Supervisor: Asst. Prof. Dr. Ali Şahin Taşlıgedik

July 2022, 66 pages

Beam-Column joints in reinforced concrete structures (RC) are important elements that connect beams and columns. For the proper transfer of lateral forces along a continuous load path, the integrity of these joints and sufficient strength are crucial. Modern seismic design philosophies dictate these joints to be designed and reinforced with the required joint shear reinforcements. Extreme principal compression stresses in these joints might cause joint shear failure even when the joints are properly reinforced considering capacity design principles. This emphasizes the significance of the axial load levels in the behavior of RC beam-column joints, which are currently being overlooked. This problem is strongly relevant to the sustainability of the modern RC structures and their expected seismic

performance since almost all existing RC buildings are susceptible to this weakness with enough axial compression levels in column. In this study, a previously developed simplified beam-column joint model, defined as an axial load-moment (N-M) interaction envelope, is implemented in the non-linear static and dynamic analyses of a modern building (with/without vertical accelerations) that suffered joint shear damage. The study aims to utilize the model in its simplest form in a widely used structural analysis software, which is expected to be used by practicing engineers. The accuracy of the joint model in simulating the seismic response is determined by comparing the analysis findings with the observations from real building damage. The model accurately represents joint shear behavior in non-linear static and non-linear dynamic analyses with varying axial load levels.

Keywords: Reinforced Concrete, Beam-Column Joint Model, Seismic performance, Non-linear Static Analysis, Non-linear Dynamic Analysis

ÖZ

MODERN BETONARME KİRİŞ-KOLON BİRLEŞİMLERİNİN BASİTLEŞTİRİLMİŞ YAPISAL MODELİN GELİŞTİRİLMESİNE YÖNELİK DAVRANIŞLARINI ANLAMAK

Şahutoğlu, Orhan
Yüksek Lisans, Sürdürülebilir Çevre ve Enerji Sistemleri
Tez Yöneticisi: Dr. Öğr. Üyesi Ali Şahin Taşlıgedik

Temmuz 2022, 66 sayfa

Betonarme yapılarda (RC) Kiriş-Kolon birleşimleri, kiriş ve kolonları birbirine bağlayan önemli elemanlardır. Sürekli bir yük yolu boyunca yanal kuvvetleri düzgün bir şekilde aktarmak için bu bağlantıların bütünlüğü ve yeterli mukavemet çok önemlidir. Sonuç olarak, modern sismik tasarım felsefeleri, bu bölgelerin tasarlanmasını ve gerekli kesme donatıları ile güçlendirilmesini zorunlu kılmaktadır. Çalışmalar, bu bağlantı noktalarında aşırı eksenel basınç gerilmelerinin, kapasite tasarım ilkeleri göz önünde bulundurularak, birleşim noktaları uygun şekilde güçlendirildiğinde bile göçmeye neden olabileceğini göstermiştir. Bu, şu anda gözden kaçırılan betonarme kiriş-kolon bağlantılarının davranışındaki eksenel yük seviyelerinin önemini vurgulamaktadır. Bu problem, modern betonarme yapıların sürdürülebilirliği ve bunların beklenen sismik performansı ile yakından ilgilidir,

ünkü neredeyse tm mevcut betonarme binalar kolonda yeterli aksenal basın seviyeleri ile bu zayıflıęa karřı hassastır. Bu alıřmada, daha nce geliřtirilmiř, aksenal yk-moment (N-M) etkileřim diyagramı olarak tanımlanan basitleřtirilmiř bir kiriř-kolon eklem modeli, eklem kesme hasarına maruz kalmıř (dikey ivmeli/dikey ivmeli) modern bir binanın doęrusal olmayan statik ve dinamik analizlerinde uygulanmıřtır. alıřma, uygulama mhendisleri tarafından kullanılması beklenen, yaygın olarak kullanılan bir yapısal analiz yazılımında modeli en basit haliyle kullanmayı amalamaktadır. Eklem modelinin sismik tepkiyi simle etmedeki doęruluęu, analiz bulgularının gerek bina hasarından elde edilen gzlemlerle karřılařtırılmasıyla belirlenir. Modelin, deęiřen aksenal yk seviyelerinde hem doęrusal olmayan statik hem de doęrusal olmayan dinamik analizlerde eklem kesme davranıřını doęru bir řekilde temsil edebildięi gsterilmiřtir.

Anahtar Kelimeler: Betonarme, Kiriř-Kolon Birleřim Modeli, Sismik Performans, Doęrusal Olmayan Statik Analiz, Doęrusal Olmayan Dinamik Analiz

To My Family

ACKNOWLEDGMENTS

The author wishes to express his heartfelt gratitude to his supervisor Asst. Prof. Dr. Ali Sahin Taslıgedik for his guidance, advice, criticism, encouragement, and insight throughout the research. His valuable guidance, advice, and care have been constructive for my self-development in academic and personal life.

I also would like to express my deepest appreciation to my parents, Sabiha and Kemal Şahutoğlu, for their unlimited support and pure love they have given me all my life. I would also like to sincerely thank my dearest sisters, Sevil and Seval Şahutoğlu, for being there. A special thank you to two of my best friends Mutlu Türk and Aydın Tuna Akyıldız, for believing in me, your support, and encouragement.

Lastly, I would like to extend my thanks to all my close friends, who are family to me, for their great friendship, support, and encouragement.

TABLE OF CONTENTS

ABSTRACT	vii
ÖZ.....	ix
ACKNOWLEDGMENTS	xii
TABLE OF CONTENTS.....	xiii
LIST OF TABLES.....	xvi
LIST OF FIGURES	xvii
CHAPTERS	
1. INTRODUCTION	1
1.1 Background and Problem Statement	1
1.2 Sustainability Perspective	4
1.3 Objective and Scope	7
2. LITERATURE REVIEW.....	9
2.1 Seismic Performance and Sustainability.....	9
2.1.1 Environmental Impacts	11
2.1.2 Economic Impacts	13
2.1.3 Social Impacts	14

2.2	Beam-Column Joint Models in Literature	16
2.3	Background Information about Beam-Column Joint N-M Representation	18
3.	METHODOLOGY.....	23
3.1	Pushover Analysis	23
3.1.1	Modeling Approach and Assumptions	24
3.2	Time History Analysis	26
3.2.1	Modeling Approach and Assumptions	27
3.3	Earthquake Data and Building Location.....	27
3.4	Building Data	29
3.4.1	Detailing of Beams and Columns.....	30
3.4.2	Non-Linear Behavior Definitions.....	32
3.5	Building Damage Observation After Earthquake.....	39
4.	RESULTS OF THE ANALYSES	43
4.1	Pushover (Non-Linear Static) Analysis Results	43
4.1.1	The Capacity Spectrum Method and Resulting ADRS	46
4.2	Time-History Analysis Results	47
4.2.1	Horizontal-1 Only and Horizontal-1 with Vertical Acceleration	48
4.2.2	Horizontal-2 Only and Horizontal-2 with Vertical Acceleration	50

4.3	Discussion of Results.....	52
5.	CONCLUSIONS	55
5.1	Limitations	58
	REFERENCES.....	59
	APPENDICES	
A.	Shear Capacity Envelopes.....	65

LIST OF TABLES

TABLES

Table 2.1. Potential impacts of RC buildings exposed to earthquake on sustainability [Gencturk, et al., 2016]	10
Table 3.1. P_t calculation for all beam-column joints with necessary parameters.....	38

LIST OF FIGURES

FIGURES

Figure 1.1. Sketch of a typical life cycle of a building [Negro, 2014]	6
Figure 2.1. Beam-column joint model examples from literature a) [Birely, et al., 2012]; b) [Unal and Burak, 2013]; c) [Favvata, et al., 2008]; d) [Youssef and Ghobarah, 2008].....	17
Figure 2.2. a) Strength hierarchy assessment example of a beam-column joint; b) Effect of column axial load amplifications [Tasligedik, et al., 2018]	20
Figure 2.3. Simplified N-M interaction envelope a) Internal RC beam-column joints; b) External RC beam-column joints [Tasligedik, 2022]	21
Figure 3.1. Hinge Assignments for exterior and interior beam-column joints	26
Figure 3.2. Acceleration time histories and Spectral Accelerations of used earthquake data.....	28
Figure 3.3. Building and earthquake stations.....	29
Figure 3.4. Details of the beams and column of the used frame	31
Figure 3.5. Moment-curvatures for push action.....	33
Figure 3.6. Moment-curvatures for pull action	34
Figure 3.7. Procedure to calculate principle tensile capacity of joints [Tasligedik, 2022].....	36
Figure 3.8. Geometric properties for external and internal beam-column joints [Tasligedik, et al., 2018]	37
Figure 3.9. Column N-M diagrams and N-M envelope representations of joints...	39

Figure 3.10. Failures from the real building [Courtesy of A.S Tasligedik 2011] ...	41
Figure 4.1. Capacity curve from pushover analysis	44
Figure 4.2. The damage observation from pushover analysis.....	45
Figure 4.3. Acceleration Displacement Response Spectra (ADRS).....	47
Figure 4.4. Results of time history analysis with only horizontal-1 and horizontal-1 with vertical acceleration	49
Figure 4.5. Results of time history analysis with Horizontal-2 and Vertical data (8.485 sec; 8.975 sec; 110 sec).....	51
Figure 5.1. Normalized joint N-M interaction envelopes with the 40% increase (dashed) and the original envelopes (grey envelope) for 22 external beam-column joints (Tasligedik 2020)	65

CHAPTER 1

INTRODUCTION

1.1 Background and Problem Statement

The design of reinforced concrete (RC) beam-column joints prior to the 1970s did not include joint shear reinforcement, which left beam-column joints vulnerable to seismic forces. The conventional seismic analysis assumes that joints remain rigid in reinforced concrete frame structures. Even if the beams and columns deform and sustain severe damage during an earthquake, the joint core remains elastic and acts as a rigid body [Pan, et al., 2017]. However, numerous experimental studies and post-earthquake investigations have revealed that beam-column joints significantly affect the earthquake response of reinforced concrete frame structures [Masi, et al., 2013; Paulay and Scarpas, 1981; Ricci, et al., 2010; Sezen, et al., 2003; Shafaei, et al., 2014]. Properly designed RC beam-column joints are now widely accepted as essential elements of earthquake-resistant design [Masi, et al., 2013; Shafaei, et al., 2014]. These elements are designed separately and reinforced with the required joint shear reinforcement to achieve adequate ductility in the presence of expected seismic forces. This is a crucial requirement in modern capacity design to ensure the strong column-weak beam concept (beam-sway mechanism). In this concept, the seismic energy should be dissipated at plastic hinges forming at the ends of beams [Irfani and Vimala, 2019]. This approach protects the critical elements required for the

structure's long-term stability from damage or collapse (i.e., columns and beam-column joints).

Depending on the axial load levels exerted, RC beam-column joints can behave mainly in two ways (or a combination of): i) principal tension mechanism at lower axial load levels; ii) principal compression mechanism at higher axial load levels. In the development of capacity design principles for RC beam-column joints, most of the chosen RC beam-column joint test specimens were chosen such that they represented the RC beam-column joints at higher elevations in buildings [Park and Ruitong, 1988]. However, as later shown by [Beckingsale, 1980], extreme column axial load levels can have a different effect on RC beam-column joint shear capacity. Therefore, considering the column axial load variations during earthquakes and among the floor levels within a given structure, it is critically important to define the RC beam-column joint shear behavior considering both mechanisms: principal tension at low axial load levels and principal compression at high axial load levels.

Currently, the significance of axial load levels in the behavior of RC beam-column joints is overlooked. Joint modeling approaches simulate joint inelastic behavior utilizing the moment-rotation relationship. Because each moment-rotation relation is determined for a specific axial load, models defined by that relation cannot accurately represent the joint response under varying axial load levels. Nevertheless, as stated, the variation of axial load levels can affect the shear capacity of the beam-column joint and, consequently, the seismic performance of modern RC buildings that are susceptible to this weakness if column axial compression levels are high

enough. This problem is highly relevant to the sustainability of modern RC buildings, which is crucial for sustainable development because the construction industry has severe environmental, economic, and social impacts on sustainability [Arukala, et al., 2019]. Moreover, the moment-rotation representation of RC beam-column joints' shear behavior is not a concept that can be readily understood and put to practical use by the practicing engineers. This is mostly due to the beam-column joints' being neither columns nor beams, which makes the moment-curvature concept and its application in beam-column joint modeling questionable. On the other hand, every civil/structural engineer is familiar with the concept of axial load (N) and bending moment (M) interaction envelope. Therefore, an RC beam-column joint model that can represent this behavior as a simplified N-M envelope carries a large potential for practical implementation by practicing engineers. Such a simplified model has recently been reported in the literature [Tasligedik, 2022].

In addition, joint model approaches with an excessive number of springs complicate the analysis and may lead to numerical convergence problems in structural analysis, making their application impractical in engineering practice. On the other hand, this study aims to solve this issue by integrating the N-M interaction model as simple as possible in the structural analysis software commonly used by practicing engineers. In this regard, recent research has shown that the RC beam-column joint shear capacity can be defined via an N-M interaction diagram [Tasligedik, 2022].

By defining the joint shear capacity as axial load(N)- bending moment (M) interaction and implementing it into structural analysis software, it is possible to observe the behavior of the beam-column joint under varying axial load levels and the resulting performance change.

1.2 Sustainability Perspective

Recently, the sustainability concept has been integrated and applied in various fields [Presley, et al., 2010]. There are legislations and policy adaptations for multiple sectors to achieve sustainability goals, particularly in developed countries [Comber, et al., 2012]. Building industries is one of those sectors because it plays a significant role in the three bottom line components of sustainability, which are environmental, social, and economical [Comber, et al., 2012; Negro, 2014; Tae, et al., 2011]. According to a report, the building sector contributes 36 percent to greenhouse gas emissions, generates 33 percent of waste, and contributes 10 percent to the gross domestic product as one of Europe's largest industrial sectors [Negro, 2014]. Also, buildings in the United States are responsible for 38% of the nation's total CO₂ emissions and 70% of the nation's total energy consumption [Tae, et al., 2011]. Therefore, the resilience of the buildings to an earthquake is a crucial aspect of sustainability since the performance of a structure during an earthquake can result in its failure, repair, or demolition, all of which have direct enormous environmental, social, and economic consequences. In a monetary sense, the costs of repairing, retrofitting, and reconstructing damaged infrastructures are high and significant.

Moreover, repairing or reconstructing a building result in the consumption of natural resources and energy as well as the production of wastes that have an impact on the environment. Under the social aspect of sustainability, the possibility of injuries and deaths caused by a damaged building are crucial considerations [Gencturk, et al., 2016]. The vast majority of the money, raw materials, and energy used in the structure's extraction, transportation, and construction could be wasted if it fails or becomes unusable before its intended lifespan [Gencturk and Hossain, 2013]. For instance, [Wei, et al., 2016] reports that the Great East Japan Earthquake of 2011 resulted in 15,889 fatalities and 1.12 million damaged buildings that needed to be repaired, costing \$122 billion, or 2.2% of Japan's GDP at the time. Moreover, this recovery process generated 26,3 million tons of CO₂ equivalent emissions, representing 2.1% of Japan's total greenhouse gas emissions in 2010. There is a strong link between seismic structural performance and sustainability. Therefore, precise evaluation of the seismic performance of a building during the design phase of new construction or the analysis phase of existing structures is essential to satisfy all aspects of sustainability.

LIFE CYCLE OF A BUILDING

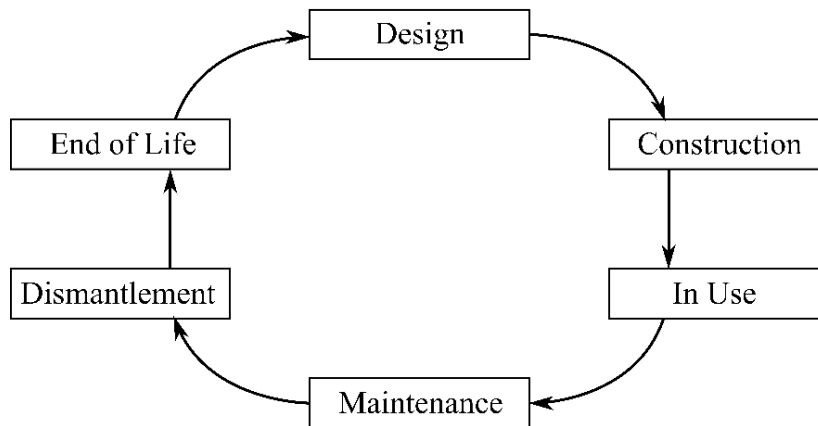


Figure 1.1. Sketch of a typical life cycle of a building [Negro, 2014]

Figure 1.1 depicts a general sketch of a building's life cycle [Negro, 2014]. As illustrated in Figure 1.1, each stage of a building's life cycle has an impact on the various aspects of sustainability. The assessment of the building's seismic performance emphasizes the majority of the stages in the life cycle. It is especially important during the design phase and before the maintenance phase. There are non-linear analysis techniques and procedures for evaluating the seismic performance of a building. These analyses require incorporating non-linear models of structural elements (beams, columns, and beam-column joints) into software for structural analysis. As stated in the introduction's first section, the axial load's effect on the behavior of the beam-column joint is currently overlooked. As a result, modern RC buildings are now vulnerable to seismic actions, as the analysis with the current joint modeling cannot consider this change in behavior caused by axial load variation. This is closely related to the sustainability of the buildings because if axial loads are not included in the modeling process, the building's response to an earthquake may

not be accurately predicted, leading to erroneous performance evaluation and design. As a result, unexpected damage and even failure may occur, requiring the building to be repaired, demolished, or rebuilt, which is not sustainable.

1.3 Objective and Scope

This study aims to implement the previously proposed simplified N-M interaction beam-column joint model [Tasligedik, 2022] into a commercial structural analysis program and observe whether the model accurately represents the seismic performance of the building, which is directly related to its sustainability. In this model, the shear capacity of a joint is represented as an axial load-bending moment (N-M) interaction envelope. Therefore, the model can represent the change in the capacity of beam-column joints subjected to varying axial loads. The model is employed in modeling a relatively modern New Zealand building as a case study. Following the 22 February 2011 Christchurch earthquake, shear failures at internal RC beam-column joints were observed in this particular RC frame building. It should be emphasized that the building was designed and detailed according to capacity design principles, and joint shear reinforcement was considerable. The beam-sway mechanism is, therefore, the expected damage mechanism following performance evaluation [Fardis, 2018]. However, post-earthquake observations did not reveal this mechanism at the internal beam-column joint. Using the N-M interaction model, non-linear static (pushover) and non-linear dynamic (time history) analyses are conducted with/without vertical accelerations. In order to evaluate the accuracy of

the model in performance assessment, the results of the analyses are compared to observations made following the 22 February 2011 Christchurch earthquake.

CHAPTER 2

LITERATURE REVIEW

2.1 Seismic Performance and Sustainability

As the energy demand for post-earthquake recovery continues to rise, discussions about how natural disasters impact the environment and, by extension, sustainability have recently gained popularity. Since earthquakes generally cause more significant damage to building structures than other natural disasters and consume the most energy in their aftermath, most of these discussions have focused on seismic hazards [Wei, et al., 2016]. When a structure sustains damage from a hazardous event, it may need to be partially repaired, discarded, and wholly replaced before reaching its anticipated lifespan [Chhabra, et al., 2018]. Due to their close connection, sustainability and earthquake resilience should be considered together [Anwar, et al., 2019]. Numerous studies and proposed methodologies exist in the literature for illustrating the relationship between sustainability and seismic performance of a building and for observing the environmental effects of earthquake damage and repair activities. Typically, these are quantified through environmental life cycle assessment (LCA) procedures [FEMA, 2018].

A building's life cycle consists of several phases: extraction of raw materials and construction, maintenance, operation, damage repair, and final disposal. Each of

these phases impacts the three main aspects of sustainability, which can be seen through the life cycle assessment [Chhabra, et al., 2018]. Potential lifetime impacts of RC buildings subjected to an earthquake on sustainability are categorized as shown in Table 2.1. As presented by [Gencturk, et al., 2016], the seismic performance of an RC building has numerous direct and indirect effects.

Table 2.1. Potential impacts of RC buildings exposed to an earthquake on sustainability [Gencturk, et al., 2016]

Environmental Impact	Social Impact	Economic Impact	
		Direct Cost	Indirect Cost
Global warming	Deaths	Material cost	Downtime
Acidification	Injuries	Construction cost	Loss of business
Eutrophication	Relocation	Operation cost	Business interruption
Eco-toxicity	Displacement	End-of-life cost	Job loss
Fossil fuel depletion	Health care disruption		Price increase
Smog formation	Psychological distress		Supply disruption
Water use	Chronic injury		
Human health risk	Family separation		
Temporary housing	Family stress		
Emergency shelter	Neighborhood disruption		

However, due to a lack of information, a life cycle assessment on the case study building for this study was not performed. Nonetheless, some case study results demonstrating the effect of seismic resilience on sustainability are presented in the following subsections under the three dimensions of sustainability (environmental, economic, and social).

2.1.1 Environmental Impacts

Building damage due to earthquakes has significant impacts on the environment. Some earthquake-related environmental impacts might be energy consumption, materials used, and emissions generated during earthquake damage repair [FEMA, 2018]. About 30% of the planet's greenhouse gasses is produced during a building's construction process. 18% of those emissions are caused by transportation and material production [Lima, et al., 2021].

Some studies in the literature use case studies of earthquake-damaged buildings to determine their carbon emission levels as a result of their repair or replacement. For instance, an eight-story case study building in an earthquake-prone area was evaluated by [Anwar, et al., 2019]. The building is subjected to various earthquake scenarios to determine the environmental effects of earthquake-caused damage at various performance levels. The building's equivalent carbon emission levels in different earthquake levels can reach 1.222×10^5 kg. Additionally, the ratio between repair and replacement costs is investigated. As indicated by the analysis results, replacement has a much greater environmental impact than repair, which has a 37.39 percent ratio at most for that building. [Chhabra, et al., 2018] conducted another case study to estimate the likely environmental impacts associated with the repair phase of a 9-story office building example. The findings show that structural components do not always cause the environmental impacts of seismic-related repair. As indicated, the equivalent CO₂ emissions for structural and non-structural components are 1,587 kg and 262,035 kg, respectively.

Using seven different earthquake data, [Gencturk, et al., 2016] provide a framework for evaluating the sustainability performance of a four-story RC structure. An environmental performance score (EPS) is utilized to determine the environmental impacts of various design levels. As robustness increases, the environmental impact ranges from 111 to over 350 EPS. According to a study, more robust designs have lower environmental impacts during repair activities even though their initial environmental impact is higher.

These case studies illustrate the environmental effects of earthquake-exposed buildings by focusing primarily on carbon emissions levels. As they demonstrate, seismic performance significantly contributed to CO₂ emissions that may result from damage repair or replacement. In addition, as previously mentioned, the building may collapse due to earthquakes. This results in greater CO₂ emissions than the repair, as demonstrated by the examples provided by studies [FEMA, 2018]. It also results in the disposal of waste. Globally, the construction industry is responsible for 45 to 65 percent of waste disposal [Lima, et al., 2021]. According to [Arukala, et al., 2019], thirty percent of India's total solid waste is generated by demolishing buildings. Numerous studies [Hossain and Gencturk, 2014; Menna, et al., 2012; Sarkisian, 2013] have been conducted on seismic damage and the importance of the seismic performance of buildings on environmental impacts.

2.1.2 Economic Impacts

The economic significance of a building's seismic performance is another important factor. Generally, economic losses are caused by either the cost of repairing or replacing structures damaged by earthquakes. Even if the structure does not collapse, it may become inoperable, which can be considered an economic impact due to the loss of rental income and relocation costs [Bird and Bommer, 2004]. For instance, [Parker and Steenkamp, 2012] represent the estimated cost of the various structures in Canterbury following the earthquake of 4 September 2010. According to a study, the estimated cost of earthquake repair and reconstruction exceeds \$30 billion. Moreover, it represented the economic losses caused by the business interruption. According to this study, earthquake damage reduces the productive capacity of numerous businesses. In addition, the earthquake reduced businesses' capacity to continue operations which led to a great impact on the economy. Some studies concentrate on case study buildings to evaluate their seismic performance and resulting economic impact. For instance, [Anwar, et al., 2019] evaluates an 8-story case study building located in an earthquake-prone region to determine the economic effects of earthquake-related damage at various performance levels. Results indicate that repair costs for that building may reach a total of \$1.71 billion. This study also investigates the ratio between repair and replacement. Under various earthquake scenarios, repair costs may reach 89.19 percent of the cost of replacement. In addition, the economic effects of earthquakes are presented in [NRC, 1992]. As one of the consequences, business interruption is described. Damage to production

equipment and loss of production materials caused by a supplier whose facilities were also damaged or inaccessibility to the facility can result in business interruption. According to a hypothetical scenario demonstrated by [Gordon, et al., 2004] that simulates the actual possibilities of an earthquake, a magnitude 7.1 earthquake in the Los Angeles metropolitan area could cost as much as \$100 billion. In this instance, the cost of business interruption exceeds the cost of structural damage. Earthquakes may have an economic impact of between \$100 million and \$100 billion, according to [Kazimi and Mackenzie, 2016].

2.1.3 Social Impacts

The social aspect of sustainability is equally as important as the environmental and economic aspects. As shown in Table 2.1, numerous impacts are documented in the literature, from deaths to neighborhood disruption. However, the most significant social factors are undoubtedly death and injuries. The seismic performance of a building plays a crucial role in ensuring the safety of those who occupy it [Gencturk and Hossain, 2013]. For example, the Great East Japan Earthquake of 2011 can be given. This earthquake alone resulted in 15,889 fatalities [Wei, et al., 2016]. [French, 2018] discusses a basic method for relating the physical earthquake damage to its social consequences. Study shows that even though the performance of structures during earthquakes has improved over the years, buildings with low seismic performance may still cause a significant number of deaths and injuries. Besides the health impacts, it also indicates that relocating from communities and neighborhoods

due to damaged residential buildings can split up families and completely destroy the social order of the neighborhood. [Kalantari, 2012] gives fatality numbers caused by earthquakes worldwide. The Tangshan earthquake of 1975 killed 200,000 people in China. Fifty-seven people died, and 8,700 people were injured in the Northridge earthquake of 1994. August's earthquake in İzmit, Turkey, resulted in 20,000 deaths in 1999. After the Gujarat earthquake of 2006, 18,000 people suffered or died in India. Additionally, in the earthquake that struck China on May 12, 2008, 400,000 people were injured, and 88,000 died or went missing. Following that earthquake, millions of people find themselves homeless. Although many factors influence the number of fatalities following an earthquake, the examples provided above can highlight the significance of the seismic performance of buildings on the social aspect of sustainability, particularly human health. In addition, some studies attempt to integrate social perspectives directly into the seismic performance and earthquake resilience design [May, 2001; May, 2007; Tanner, et al., 2020].

2.2 Beam-Column Joint Models in Literature

The behavior of RC beam-column joints and their models have been researched in numerous studies. Researchers have studied these elements to understand their behavior better, represent their flexibility, and incorporate them into seismic analysis and design processes.

Multiple models have been proposed in the literature. Some of the model examples are illustrated in Figure 2.1. For instance, Birely, et al. [2012] developed a joint model using series-connected rotational springs to represent the beam and the joint responses, as shown in Figure 2.1a. In this study, the moment-rotation relationship is used to define rotational springs. The beam spring was established using laboratory data from frame tests, whereas the joint response is characterized by the bilinear shear stress-strain relation being transformed into a moment–rotation relationship.

Similarly, Unal and Burak [2013] aimed to create a joint model to be integrated into the commercial structural analysis software. In this particular model, shown in Figure 2.1b, the joint is characterized as rotating springs, in which inelastic behavior is simulated using the moment-rotation relation. Rotational springs are attached to the panel zone, comprised of rigid connections that connect beams and columns. The model is validated by comparing the analytical results with the experimental results. Kim and LaFave [2007] evaluated the parameters that affect joint shear behavior, including column axial load. According to this research, column axial compression is only beneficial for joint shear strength when there is insufficient transverse joint shear reinforcement. It also shows that the column axial compression effect on joint

shear capacity cannot be clearly represented since, in the database utilized in this study, joint shear capacity is controlled by horizontal joint shear reinforcement/strength. Similar RC beam-column joint models are reported in the literature [Borghini, et al., 2016; Elmersi, et al., 2000; Favvata, et al., 2008; Youssef and Ghobarah, 2008].

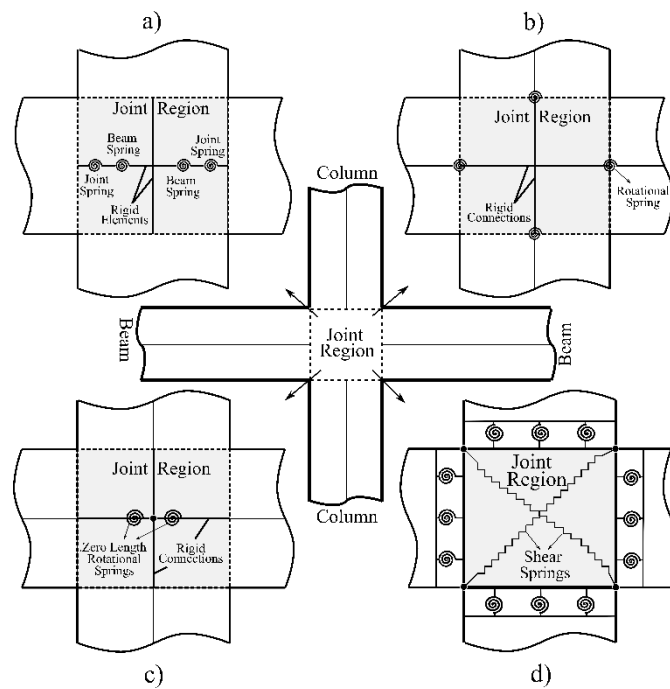


Figure 2.1. Beam-column joint model examples from literature a) [Birely, et al., 2012]; b) [Unal and Burak, 2013]; c) [Favvata, et al., 2008]; d) [Youssef and Ghobarah, 2008]

These research examples demonstrate that current joint modeling approaches either employ non-linear rotational springs defined by the moment-rotation relationship or consider a broad range of design parameters governing joint behavior. In addition, given that the axial load levels are expected to vary at each floor level during seismic action, it becomes critical to represent this variation in the beam-column joint

elements. However, the models in the literature are mostly defined based on moment–rotation response defined under constant axial load levels. As a result, they cannot accurately represent the response under varying axial load levels. This significantly hinders their ability to represent/simulate the real behavior of the RC beam-column joints.

2.3 Background Information about Beam-Column Joint N-M Representation

The N-M interaction diagram representation of the RC beam-column joint is a concept derived from the strength hierarchy method. In this method, the capacities of structural elements (columns, beams, beam-column joints) are represented as a function of axial load and bending moment at the corresponding joint. Similarly, demands are also shown on the same diagram, allowing for a comparison between the capacity and demand of these structural elements in response to lateral actions. Structural elements may fail consecutively in each beam-column connection if their capacities are insufficient to meet the demand. By modeling demand and capacity on the same domain, the strength hierarchy method allows one to observe the sequence of failure and determine the weakest structural element on the corresponding joint [Tasligedik, et al., 2018]. When this procedure is applied for RC beam-column joints' shear capacity, one obtains N-M envelopes, as shown in Figure 2.3. This figure identifies critical points via the strength hierarchy assessment method. Figure 2.2 illustrates the results of a strength hierarchy assessment of a beam-column joint

in its simplest form. The lower bound shear capacity of the joint, which corresponds to the joint's principal tensile capacity, is determined by utilizing the longitudinal and transverse steel reinforcement provided within the joint. The total principal tensile capacity (P_{tt}) is determined by adding the contribution of the concrete in the beam-column joint, i.e., without joint shear reinforcement, to the contribution of the provided reinforcements. The principal compression strength defines the upper bound for the reinforced concrete beam-column joints reinforced with shear reinforcement (P_c). For the sake of simplicity, Figure 2.2 does not include a representation of the beam capacity. The numbers where capacities overlap with the demand representation indicate the order of failure of the connected structural elements, starting with the initial failure and ending with the final failure, respectively. In Figure 2.2a, the demand curve coincided with the joint capacity's lower bound, indicating that the principal tension mechanism governs the joint's expected failure mode. However, excessive amplification of the axial force may cause a shift in the joint response and change the joint's expected failure mode. The possible behavior change is depicted in Figure 2.2b. Although the principal tension mechanism was previously the governing behavior, the first intersection occurs with the upper bound of the joint shear capacity representation due to an axial load increase in the demand curve, in which the principal compression mechanism becomes the governing behavior.

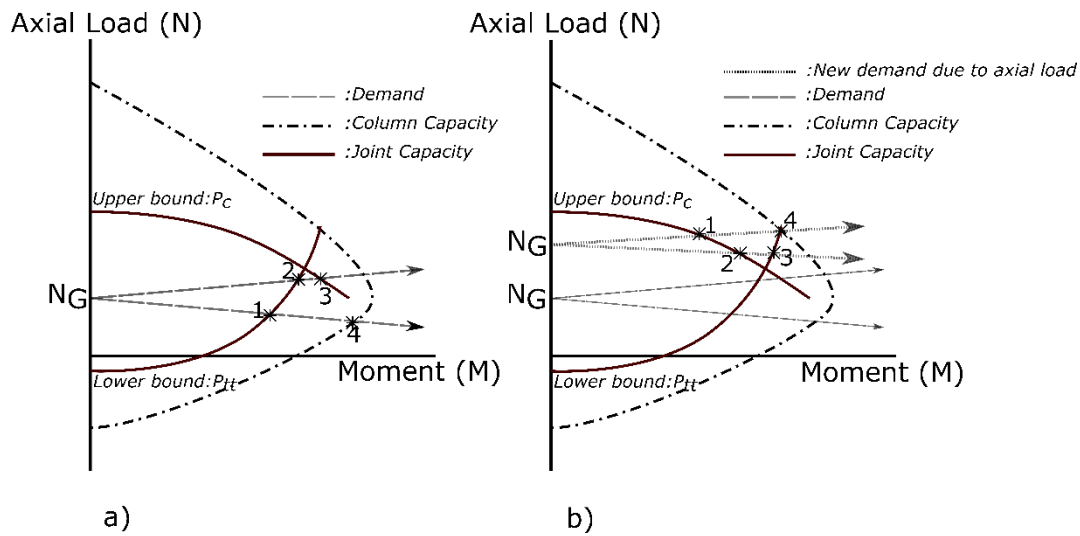


Figure 2.2. a) Strength hierarchy assessment example of a beam-column joint; b) Effect of column axial load amplifications [Tasligedik, et al., 2018]

As shown in Figure 2.2, the representation of joint shear capacity creates an envelope curve. It has been proposed that the envelope can be simplified by identifying tree-typical points [Tasligedik, 2022]. This study uses a simplified N-M diagram rather than the envelope derived from the strength hierarchy assessment. This is because the simplified N-M diagram can be created using more straightforward calculations by only defining three points. It is also easier to incorporate into software for structural analysis, which is one of the aims of this research.

In the simplified N-M interaction envelope representations of the RC beam-column joints, three points can be identified, as shown in Figure 2.3: The first point, designated N_1 , is determined in the manner depicted in Figure 2.3 (analogous to uniaxial compression). The second point (N_2) is determined in the same manner as shown in Figure 2.3 (analogous to uniaxial tension). It should be noted that research

[Tasligedik, 2022] has shown that the conservative capacity estimation for N_2 value in internal beam-column joints closely estimate the behavior of internal RC beam-column joints, while it underestimates the behavior of the external RC beam-column joints. Therefore, the research reported in this article chooses an un-conservative N_2 value in external beam-column joint. Point 3 (N_3, M_3) is a corner location having equivalent principal compression and tension capacities, analogous to the balanced case in the N-M diagram for columns. The necessary equations for calculating the corner location have been defined utilizing concepts of strength hierarchy assessment [Tasligedik, 2022]. An example of the beam-column joint N-M interaction envelope is explained in more detail in the methodology part

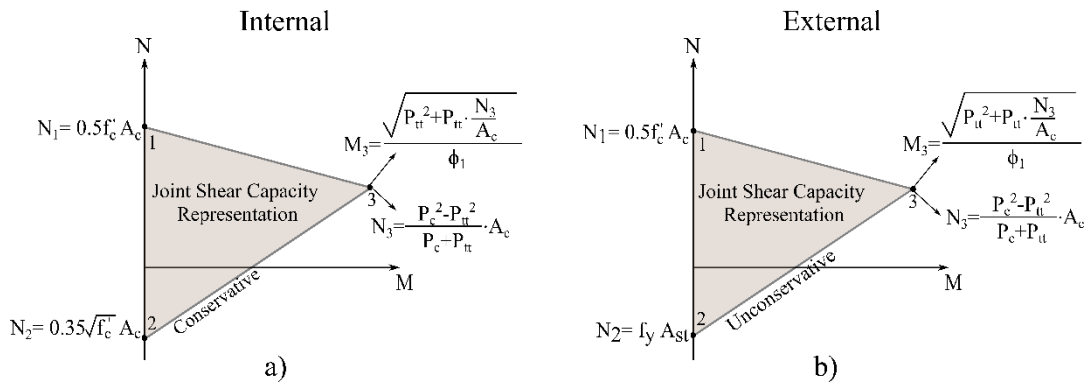


Figure 2.3. Simplified N-M interaction envelope a) Internal RC beam-column joints; b) External RC beam-column joints [Tasligedik, 2022]

CHAPTER 3

METHODOLOGY

A modern RC frame building in Christchurch, New Zealand, is chosen as a case study example since joint shear failures were observed at its internal beam-column joints. The purpose of the analyses is to numerically assess the non-linear behavior and the structure's seismic performance using the earthquake data that caused the observed damage. Non-linear static (pushover) and non-linear dynamic (time history analysis) analyses with/without vertical accelerations are performed using the mainstream structural analysis software SAP2000 by implementing the simplified N-M interaction joint model within the structural model. Pushover analysis is less time-consuming and easier to carry out than time history analyses. However, time history analysis is a more comprehensive method for simulating a building's response to an earthquake [Çavdar and Bayraktar, 2013]. Both analyses are conducted to determine the model's accuracy and applicability in engineering practice.

3.1 Pushover Analysis

The pushover method, a non-linear static procedure, can estimate seismic structural deformations. It can be used to evaluate the seismic capacity of existing structures in a number of recent retrofit seismic design guidelines. It can also be used to improve the performance of new buildings that rely on ductility or redundancy to withstand

earthquake forces[Khan, 2013]. The front side frame of the building, which has the majority of the reported joint shear damage, is modeled using SAP2000 for pushover and time history analyses. Following the description of the properties of each segment, a two-dimensional model of the frame is created. The dead weight of each column and beam on each floor level is computed and evenly distributed to each beam on the corresponding floor as dead load. In the absence of information regarding the interior of the building, a live load of 3kN/m^2 is assumed per New Zealand standards [NZS 4203:1992]. In addition, the safety factor is not applied for the dead and live loads. Assumption of the mass distribution is made by the tributary area concept. The estimated masses are distributed equally across each joint on that level on the 2D frame.

3.1.1 Modeling Approach and Assumptions

The non-linear behavior of each element is defined using plastic hinge at the corresponding joint. The moment-rotation relationship is used to model the non-linear behavior of beams. On the other hand, non-linear column behavior is modeled using the axial load-moment interaction (N-M) in the plastic hinge regions. Beam-column joint behavior is modeled using the developed N-M interaction model, implemented as N-M user-defined hinges in the software. Joint regions are modeled and connected with rigid elements to the beams and columns. Plastic hinges are defined at the intersection point of rigid elements and structural members. Joint plastic hinges are defined on the columns below the corresponding joint because the

joint model derived from the strength hierarchy assessment represents the joint shear capacity below the joint panel region [Tasligedik, et al., 2018]. As a result, each column has two N-M interaction hinges, one for the column and one for the joint response. It is also possible to define plastic hinges for columns and joints in series. However, this was found unnecessary in this study since the column capacity often covers a larger region, indicating that it is higher than the joint capacity, and the application is kept as simple as possible for practical purposes.

Figure 3.1 illustrates an example of hinge assignments for exterior and interior beam-column joints, together with details about the non-linear behavior of each structural element (i.e., M- ϕ for beams and N-M for columns and joints) and implementation to the software. In this context, the moment, curvature, and axial load are represented by the symbols M, ϕ , and N. In the pushover analysis, the performance point was determined through the Capacity Spectrum Method (CSM) [ATC-40, 1996], considering the acceleration-displacement response spectrum (ADRS) from the nearest earthquake station.

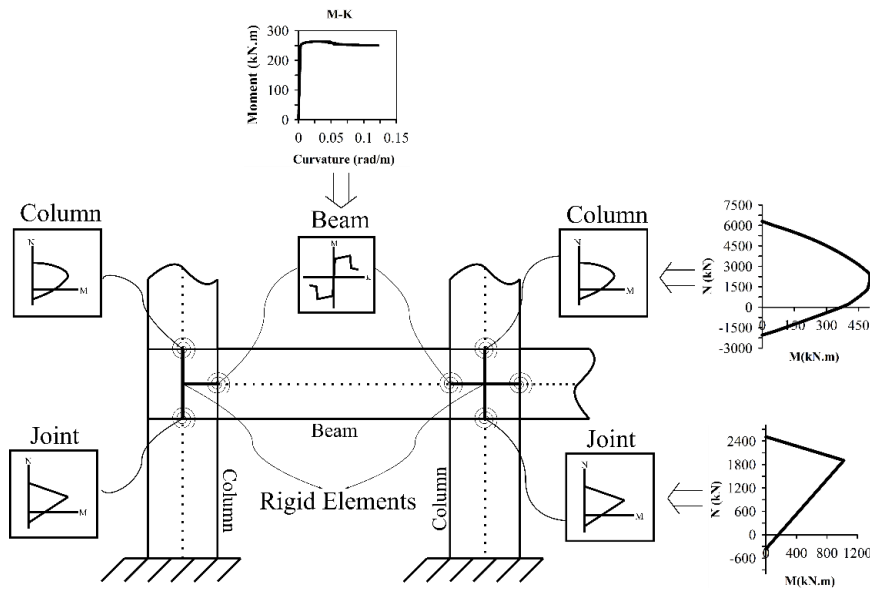


Figure 3.1. Hinge Assignments for exterior and interior beam-column joints

3.2 Time History Analysis

Time history analysis can be used to examine a structure's time-varying dynamic response to a specified loading. The seismic response of a structure can be determined using time history analysis based on the dynamic loading of representative earthquakes [Patil and Kumbhar, 2013]. In the non-linear time history analyses, the same model developed for the pushover analysis is utilized. Since the studied building experienced the 22 February 2011 Christchurch Earthquake in New Zealand, the ground motion data is obtained from the nearest station to the location of the building (REHS Station). More details about the ground motion and damage observation data are given in the Earthquake Data section and the building data section, respectively.

3.2.1 Modeling Approach and Assumptions

The analyses are carried out using three separate time history functions defined in the software: two horizontal and one vertical. In the first analysis case, the building model is subjected to only horizontal ground accelerations. In the second analysis case, simultaneous horizontal and vertical ground accelerations are applied to the model to simulate the true response as accurately as possible to observe the effects of the experienced ground motion. The building had four seismic frame systems in both x&y directions. Since the analyses carried out are in 2D and on only one of the four seismic frames, the input ground motion had to be scaled by 1/4, assuming each lateral seismic framing system encounters one-fourth of the seismic forces.

By simultaneously applying horizontal and vertical ground acceleration, it is possible to observe the effect of vertical acceleration on the building response while accounting for the effect on the axial load variations. For the sake of simplicity, P-Delta effects are neglected, and the damping ratio is set to 5%.

3.3 Earthquake Data and Building Location

The 22 February 2011 earthquake in Christchurch, New Zealand, had an $M_w=6.1$ magnitude and 5 km depth. The ground motion data is obtained from an article that includes data from 20 strong-motion stations situated throughout the Christchurch region [Bradley and Cubrinovski, 2011]. The Christchurch Resthaven (REHS) station is the closest station to the building. Figure 3.2 shows the acceleration time

histories and the spectral acceleration vs. period graphs obtained from this station.

Spectral accelerations are shown obtained with a 5% damping ratio.

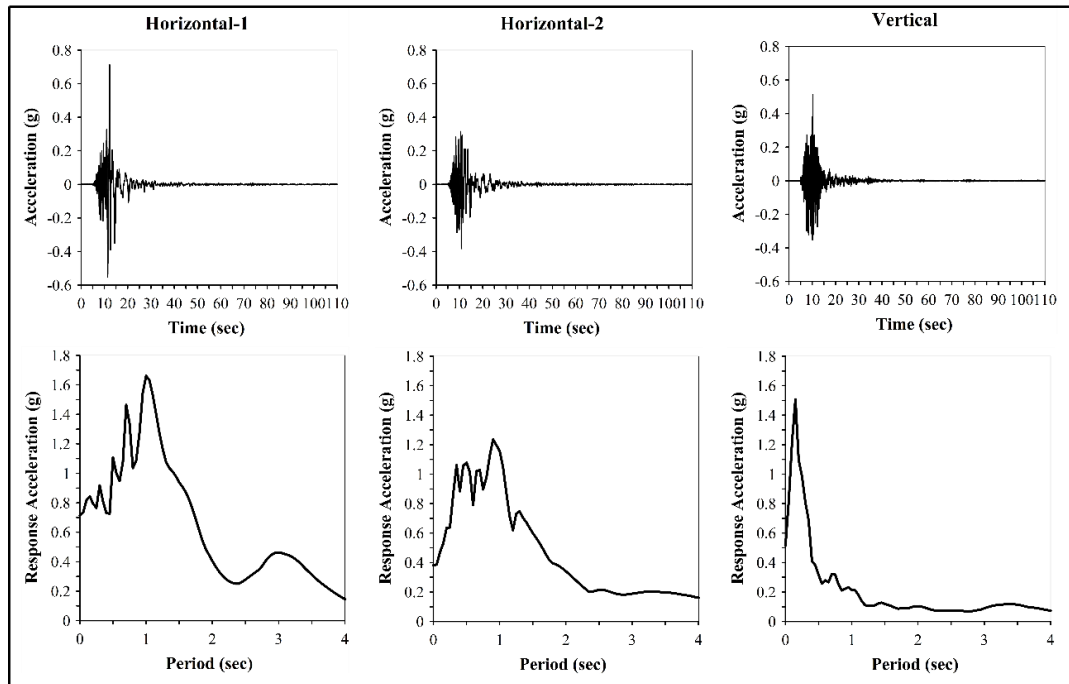


Figure 3.2. Acceleration time histories and Spectral Accelerations of used earthquake data

As previously mentioned, the earthquake's depth was 5 km, and the ground motion corresponds to a 9 km distance from the structure. As illustrated in Figure 3.2, the horizontal peak ground accelerations (PGA) obtained from REHS station records range between 0.4g and 0.7g. In contrast, the peak vertical ground acceleration (PGAv) recorded is approximately 0.5g. Seven of the twenty earthquakes with data from separate stations have observed peak vertical accelerations of more than 0.6g; in fact, significant values such as 2.21g and 1.88 g have been detected throughout

the region [Bradley and Cubrinovski, 2011]. Those vertical ground accelerations are very high. Mentioning that these vertical ground accelerations are rare, vertical, and horizontal peak acceleration ratios of the ground motion are also uncommon. This makes the case study unique. Figure 3.3 depicts the location of the building and the stations on a map. Although just the nearest station's data is used, two other stations (PRPC, CCCC) locations are shown because both are pretty close to the building's location and have recorded peak vertical ground accelerations in the range of 0.79g-1.88g.

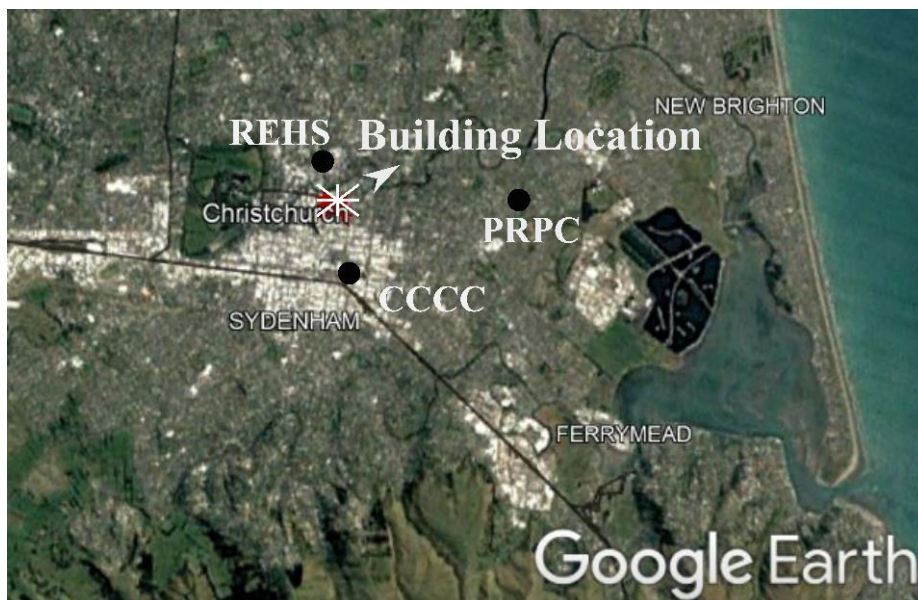


Figure 3.3. Building and earthquake stations

3.4 Building Data

The case study structure is a seven-story reinforced-concrete frame building designed according to capacity design principles.

3.4.1 Detailing of Beams and Columns

Details of all beams and columns and material properties are shown in Figure 3.4. Columns up to the fourth floor have identical detailing and are reinforced with intermediate steel along each section side, whereas columns between the fourth and seventh floors have the same detailing but lack intermediate reinforcement. Considering the amount of intermediate longitudinal steel and types of stirrups, each beam-column joint has identical details to the column below the corresponding joint. Therefore, beam-column joints on the first through fourth floors have the same stirrup type and four intermediate longitudinal steels, as shown in Figure 3.4. Figure 3.4 further shows that there is no intermediate longitudinal reinforcement between the 5th and 7th-floor columns. Also, the joints on these floor levels lack intermediate steel. Additionally, the number of transverse reinforcement sets in the joint region varies only on the first floor. On the first floor, beam-column joints have four sets of transverse reinforcement, while the remaining floors have five sets corresponding to the type of stirrups used on the column below the relevant beam-column joint. Except for the first floor, all beams have the same dimensions. On the other hand, reinforcement details vary according to the floor level, as well as the connection of the beams to internal or external columns. In Figure 3.4, f'_c represents the concrete's compressive strength, f_y and f_{yw} represent the longitudinal and transverse reinforcement's yield strengths, respectively. ϕ_s represents the diameter of the transverse steel.

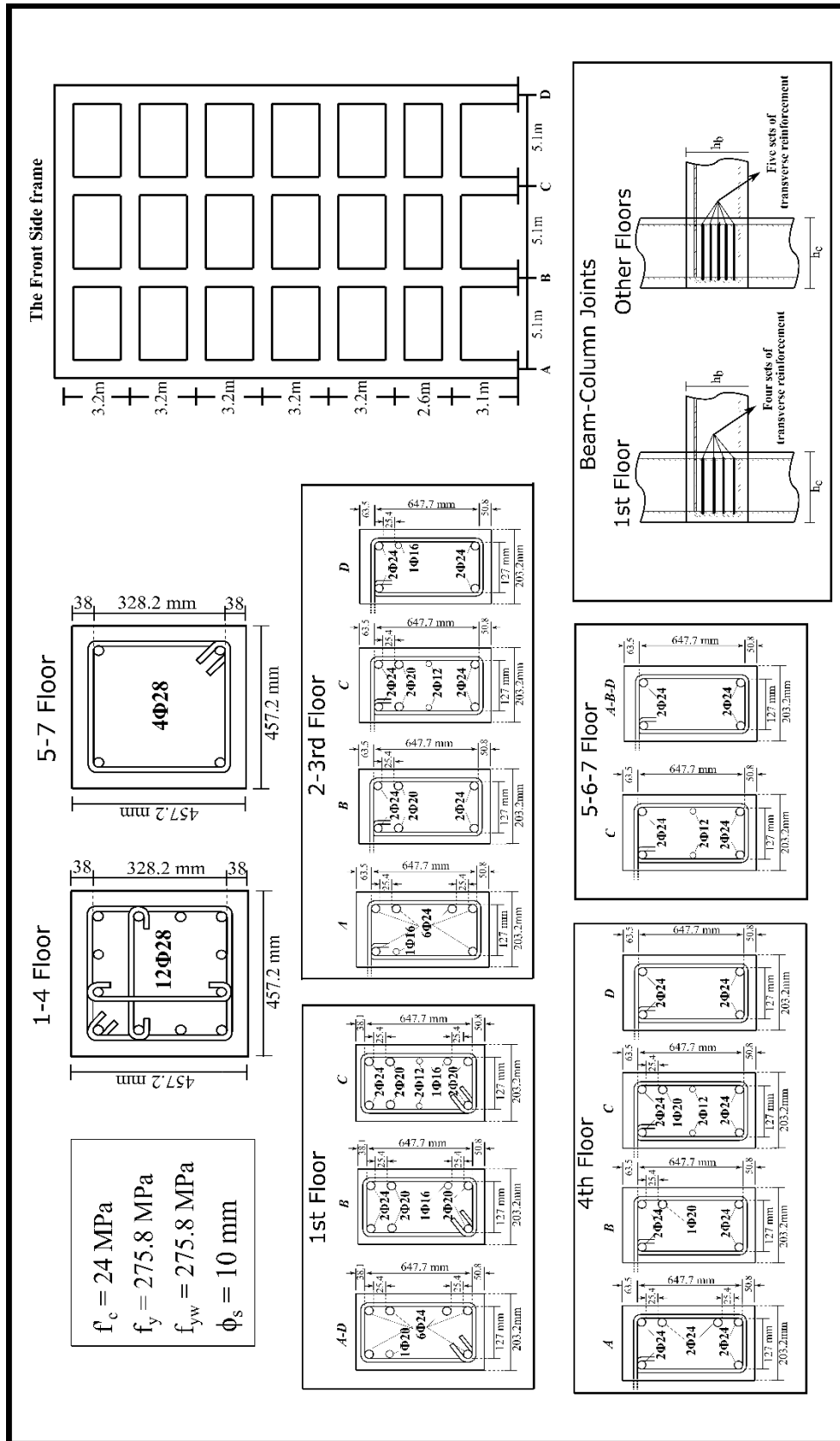


Figure 3.4. Details of the beams and column of the used frame

3.4.2 Non-Linear Behavior Definitions

3.4.2.1 Beams

Beams' non-linear behavior is defined by the moment-curvature relation obtained using Excel spreadsheets containing the Tri-linear steel model and the Modified Kent and Park model for concrete [Ersoy, et al., 2003]. These programs are used to determine yielding and ultimate curvature and moment values, which are then integrated into the structural analysis software following FEMA 356 guidelines. In addition, the length of a plastic hinge is calculated using $0.5H$, the simplest form of plastic hinge length [Park and Paulay, 1975]. In the formula for plastic hinge length, 'H' represents the section depth. Several beams feature asymmetrical reinforcements on the tension and compression sides of the beam section, resulting in a different $M-\phi$ diagram depending on the direction of the lateral force. Figure 3.5 and Figure 3.6 show the resulting representation of the moment curvatures for both push and pull actions, respectively. In the figures, each letter denotes a particular column, and each number denotes the floor level, whereas the letters L and R denote the beams' left and right connections. For instance, 'b4,L' denotes the beam's moment-curvature connecting to the second joint's left side on the fourth floor.

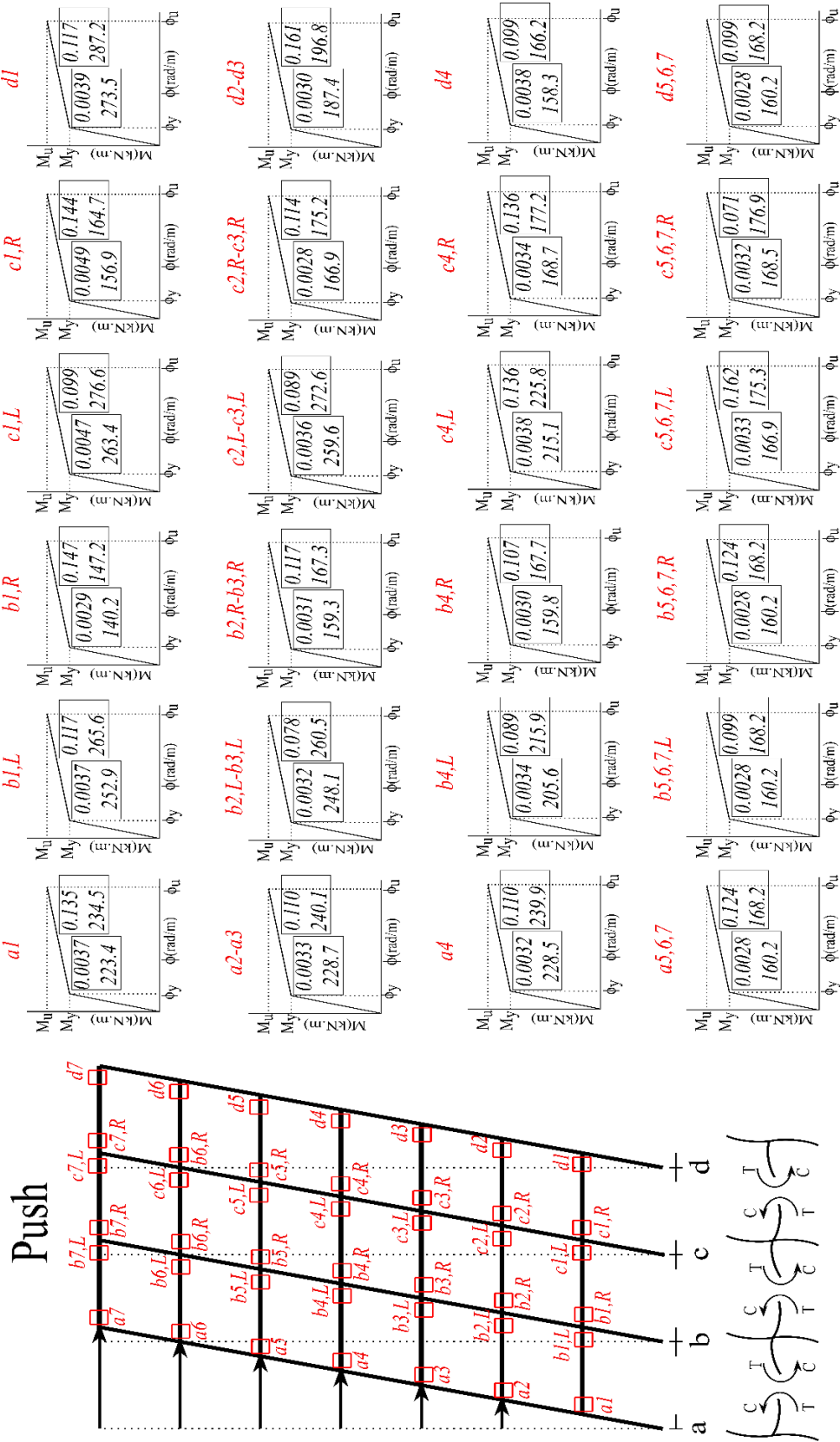


Figure 3.5. Moment-curvatures for push action

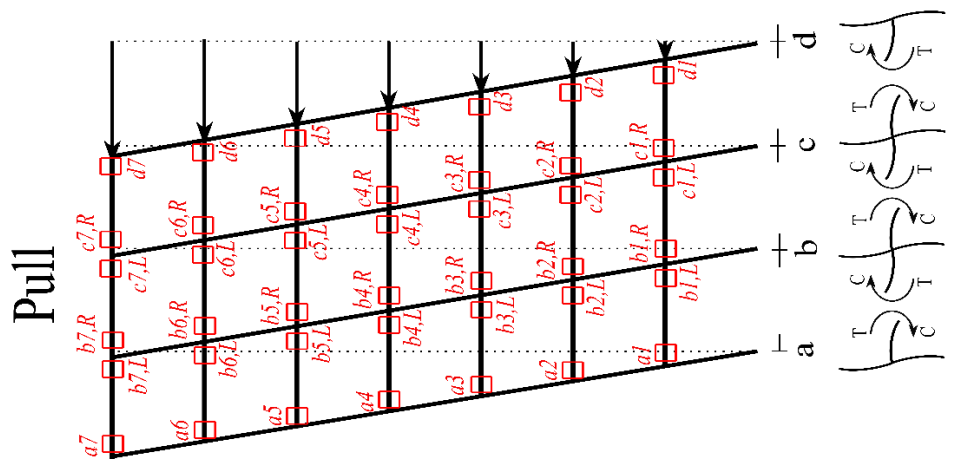


Figure 3.6. Moment-curvatures for pull action

3.4.2.2 Columns

Column capacities are described in terms of the axial load-moment interaction (N-M). Because the column details are identical between the 1st and 4th-floor levels and between the 4th and 7th-floor levels, only two distinct N-M diagrams are formed, as summarized in Figure 3.9.

3.4.2.3 Beam-Column Joints

The N-M interaction capacity representations for the beam-column joints are calculated using the equations shown in Figure 2.3, where three points form an envelope representing joint shear capacity. Figure 3.7 and Figure 3.8 describe and show the variables and procedures required to obtain those points forming an envelope. The first phase of the process depicted in Figure 3.7 illustrates the total horizontal capacity contribution of the transverse reinforcement set (F_{wx}) and the total vertical capacity contribution of the intermediate longitudinal steel in the columns (F_{wy}). Equations are multiplied by the integers n and m , representing the total number of sets of transverse reinforcement in the joint and the total number of intermediate steels in the column, respectively (e.g., the joint illustrated in Figure 3.7 has $n = 5$ and $m = 2$). Θ indicates the approximate diagonal cracking angle on the joint panel, which only depends on the beam-column geometric properties. As stated in the procedure's second stage, an equivalent diagonal tension force (F_{jts}) is obtained. Finally, total principal tension capacity (P_{jt}) can be computed by adding the principal tension capacity provided by steel reinforcements (P_{ts}) within the joint,

which is calculated as shown in Figure 3.7, to the principal tension capacity of the joint without joint shear reinforcement (P_t). P_t is obtained based on empirical formulations as reported/summarized in the related publication and taken as $P_t = 0.29 \sqrt{f'c}$ in this study [Tasligedik, et al., 2018].

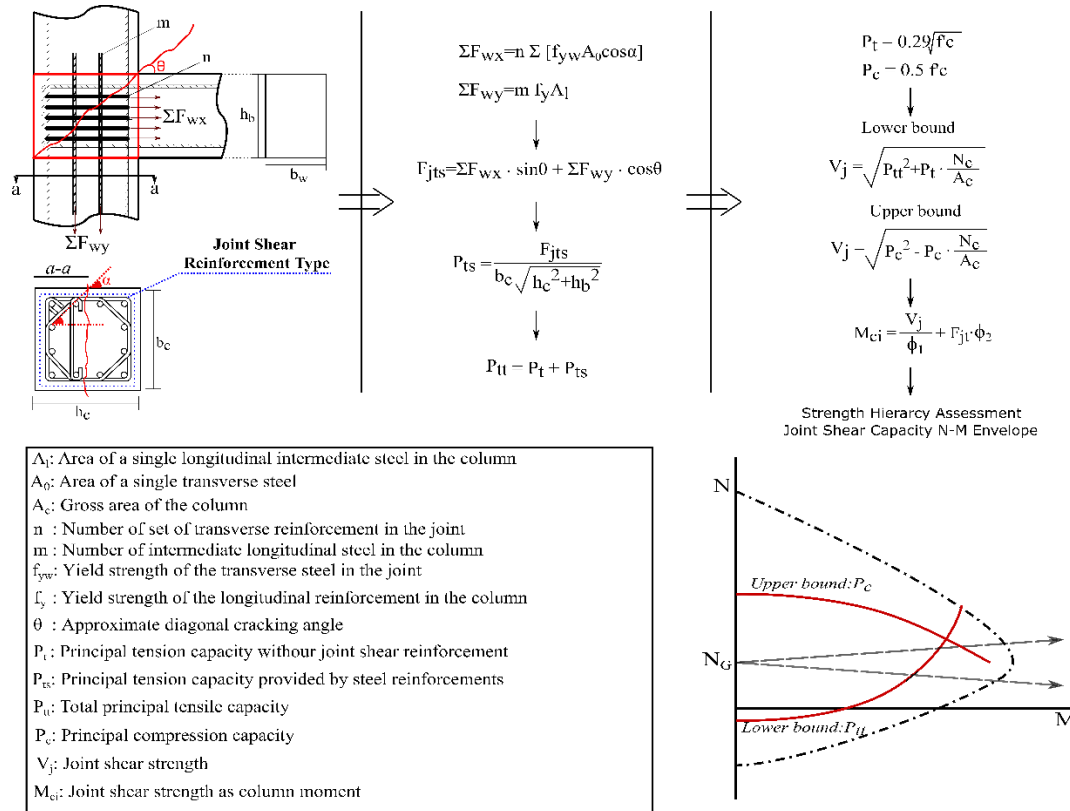


Figure 3.7. Procedure to calculate principal tensile capacity of joints [Tasligedik, 2022]

The calculated P_{tt} value is then substituted into the equations shown in Figure 2.3. As it can be seen, the corner moment value at point three (M_3) has a ϕ_1 coefficient in the denominator of the equation (geometric coefficient). This coefficient is different for external and internal beam-column joints and is calculated using the geometric properties presented in Figure 3.8 [Tasligedik, et al., 2018].

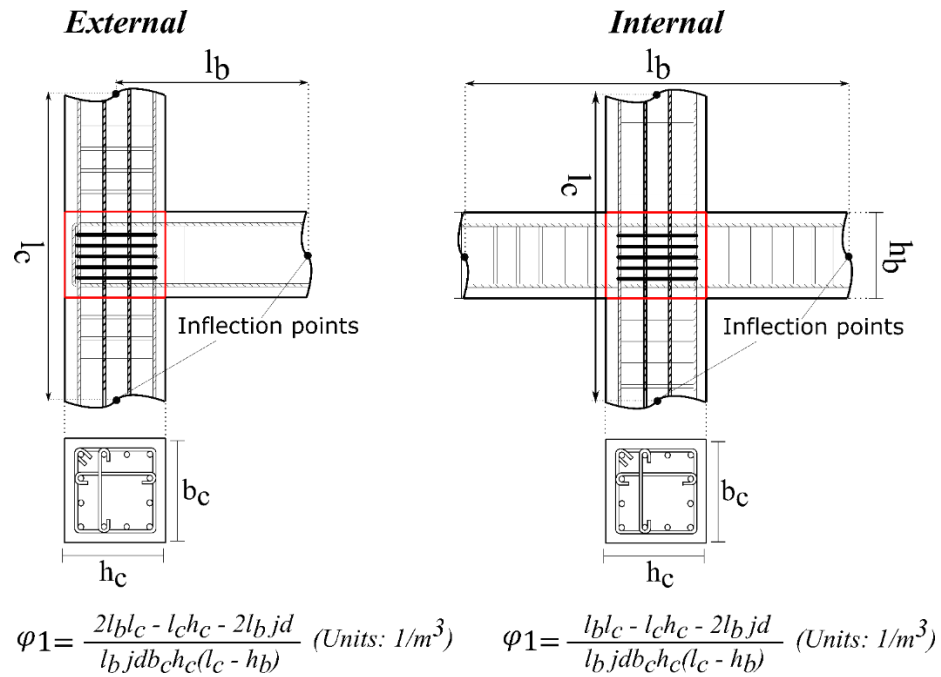


Figure 3.8. Geometric properties for external and internal beam-column joints [Tasligedik, et al., 2018]

As mentioned in the background section, the shear capacity of each joint is represented as a simplified N-M interaction diagram and implemented in the software. The representation of joint shear capacity as a simplified N-M interaction closely matches experimental observations for internal beam-column joints. On the other hand, this representation conservatively estimates the expected capacity in external beam-column joints. Therefore, the capacity representation as simplified N-M for internal beam-column joints is used as reported in the literature. In comparison, the representation for external beam-column joints in the respective N-M representation charts is increased by 40% at the corner capacity point. The justification for this 40% correction is illustrated in appendix 1 using the 22 beam-column joints test data found in the literature. Figure 5.1 in the appendix contains

data sets illustrating the shear capacity envelopes of 22 external beam-column joints with and without the assumed 40% capacity increase. As seen in this figure, this modification facilitates a more accurate correlation between the N-M capacity representation of external beam-column joints and the observed behavior from the database. Accordingly, the N-M envelope of each beam-column joint is obtained and summarized in Figure 3.9. The parameters and final P_{tt} values for each beam-column joint in the building that are utilized to generate N-M envelopes are listed in Table 3.1.

Table 3.1. P_{tt} calculation for all beam-column joints with necessary parameters

Floor No	Ext/Int	Θ	f_{yw} (Mpa)	A_0 (mm ²)	f_y (MPa)	A_1 (mm ²)	ΣF_{wx} (N)	ΣF_{wy} (N)	F_{jts} (N)	P_t (MPa)	P_{ts} (MPa)	P_{tt} (MPa)
1	Ext & Int	58.17	275.79	78.5	275.79	615.8	259794	679326	579003	1.421	1.461	2.881
2-3-4	Ext & Int	59.04	275.79	78.5	275.79	615.8	324743	679326	627949	1.421	1.546	2.966
5	Int	59.04	275.79	78.5	275.79	615.8	216495	339663	360387	1.421	0.887	2.308
6-7	Int	59.04	275.79	78.5	275.79	0	216495	0	185651	1.421	0.457	1.878
4-5-6-7	Ext	59.04	275.79	78.5	275.79	0	216495	0	185651	1.421	0.457	1.878

		n	m	h_c (mm)	b_c (mm)	h_b (mm)
1	Ext & Int	4	4	457.2	457.2	736.6
2-3-4	Ext & Int	5	4	457.2	457.2	762
5	Int	5	2	457.2	457.2	762
6-7	Int	5	0	457.2	457.2	762
4-5-6-7	Ext	5	0	457.2	457.2	762

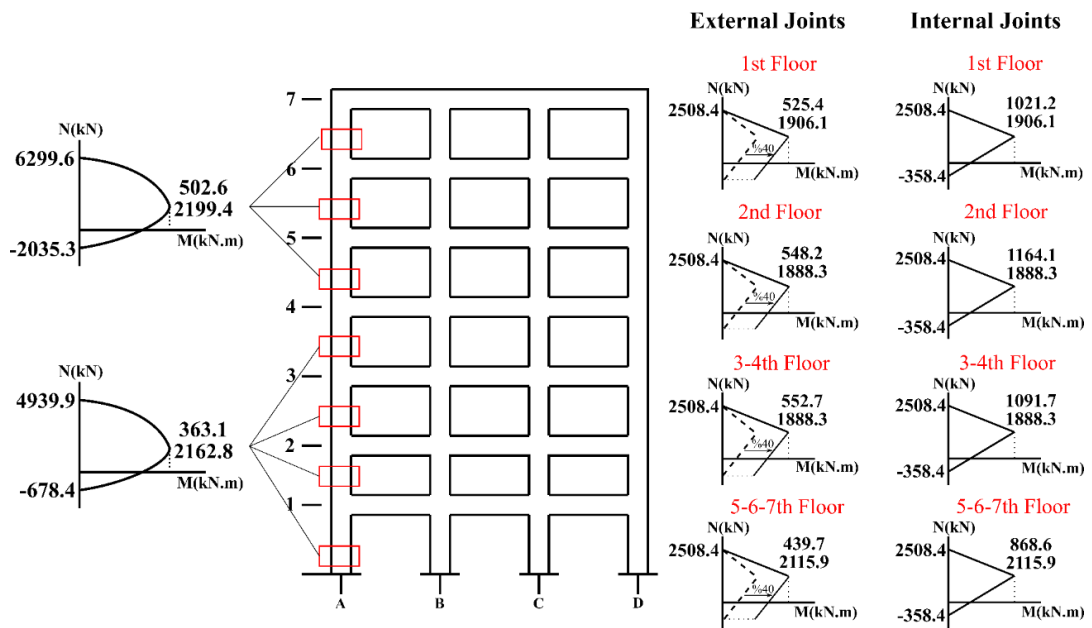


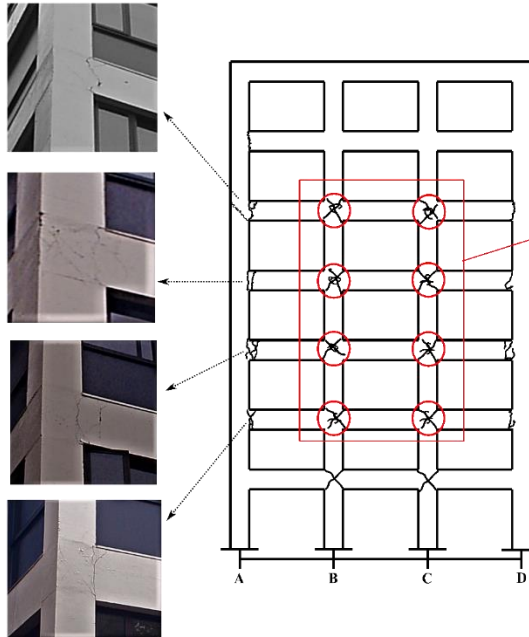
Figure 3.9. Column N-M diagrams and N-M envelope representations of joints

3.5 Building Damage Observation After Earthquake

Since this case study building was designed according to capacity design principles, the beam-column joints were adequately reinforced with transverse reinforcement. However, the structure experienced an unusual pattern of damage that could not be explained with the capacity design principles. Figure 3.10 contains photographs taken during the structural examinations in New Zealand that depicts the observed damage on the building's front frame, the utilized part of the structural framing system in the analyses reported in this article [Tasligedik 2011]. The main damage observation was predominant shear damage at all internal beam-column joints from 1st to 5th-floor levels. No plastic hinge formation was observed at the connected beams and columns at those internal beam-column joints.

It should be noted that although capacity design principles ensure beam-sway mechanism (strong column-weak beam analogy), joint failures occurred on the internal joints rather than the expected plastic hinge formation on the beam ends. On the other hand, there was no joint shear damage at any external RC beam-column joints except on the fifth floor. In the closer perspective depicted in Figure 3.10, one diagonal crack formation can be noticed running from the joint's top left corner to its bottom right corner. Additionally, the beams attached to the external beam-column joints exhibited mainly flexural cracks where they were connected, but no wholly developed plastic hinge was seen. Some joint shear damage was observed at the external beam-column joints on the left side of the structural frame, but the flexural cracks at the connected beams seemed more predominant. Therefore, the main damage type observed in the external beam-column joints was the initiation of beam plastic hinging. Only the beam plastic hinge formations on the left side of the frame are illustrated in greater detail (using the limited photographic records of the structure); however, plastic hinges on the right side of the frame can also be seen from the frame demonstration.

Beam Plastic Hinges



Joint Shear Failures

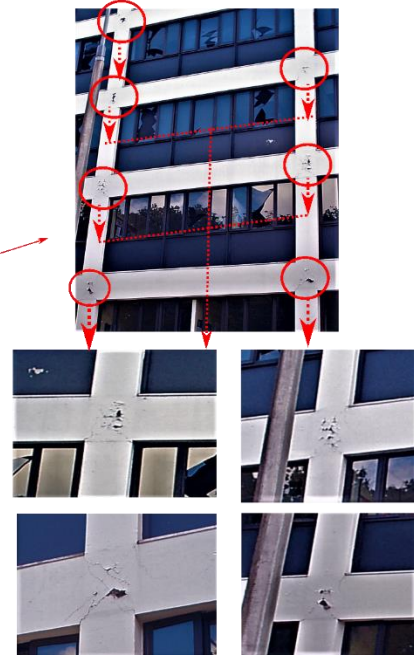


Figure 3.10. Failures from the real building [Courtesy of A.S Tasligedik 2011]

CHAPTER 4

RESULTS OF THE ANALYSES

4.1 Pushover (Non-Linear Static) Analysis Results

Displacement-controlled pushover analysis is performed in the structural analysis software SAP2000. Equivalent static forces are applied at each floor level in a reverse triangle distribution. The capacity curve, which shows the base shear versus roof displacements, is obtained as shown in Figure 4.1. The damage revealed throughout specific essential steps of the non-linear static analysis is depicted in Figure 4.2. The analysis results using the proposed joint model were similar in many respects to the observations made in the real structure following this earthquake.

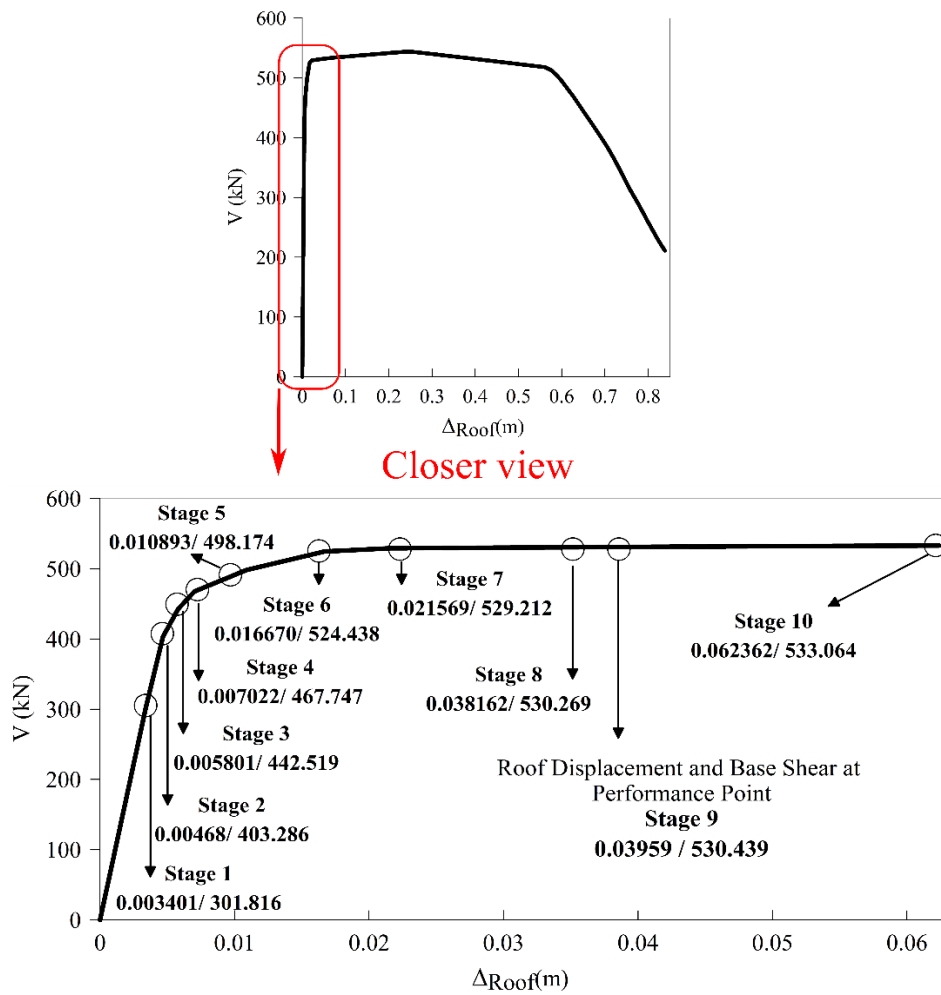


Figure 4.1. Capacity curve from pushover analysis

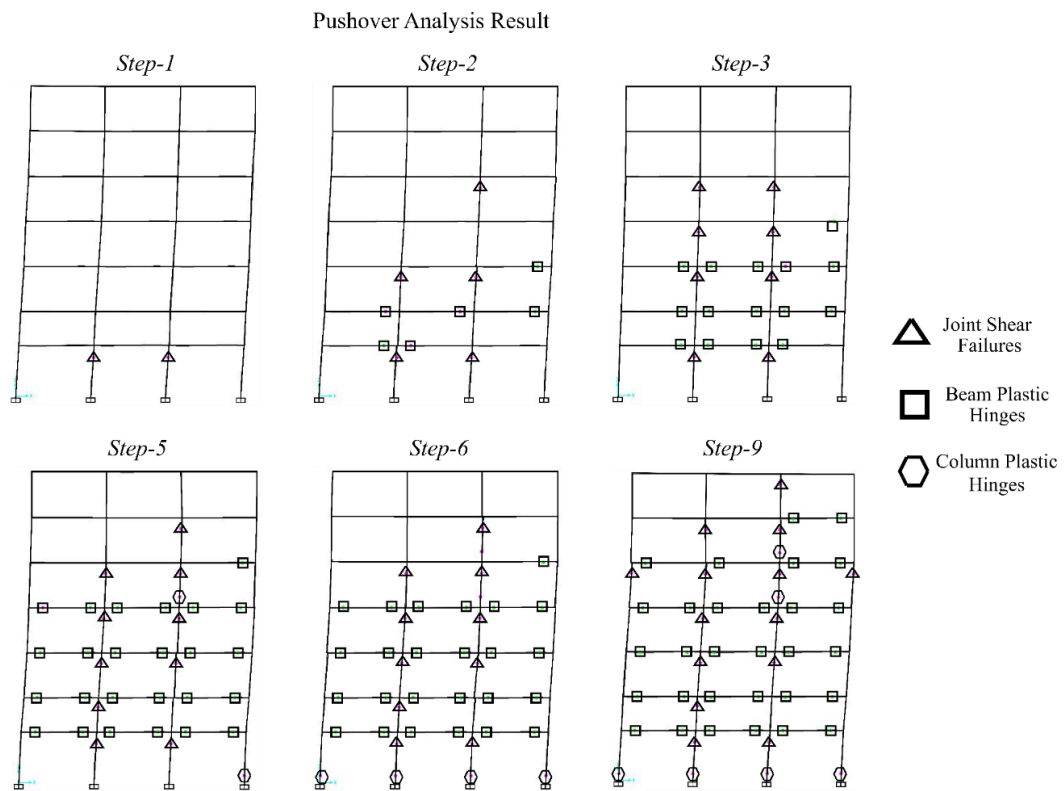


Figure 4.2. The damage observation from pushover analysis

According to the results reported in Figure 4.2, the initial stage of the analysis (Stage1) shows joint failures at the internal beam-column joints of the first-floor level. In the following stage (Stage 2), more internal joint failures and beam plastic hinges are identified. In Stage 3, joint failures at most internal RC beam-column joints from the first to the fifth-floor levels develop. Stage 5 illustrates all the internal joint shear failures except for the second floor's right internal joint, whose connected beam develops plastic hinging before the joint could fail in shear. It should be noted that all other joint shear failures at the internal beam-column joints occurred prior to the formation of plastic hinges on the connected beams to those joints. The next stages illustrate more failure patterns forming on the structure until the performance

point is reached, which corresponds to the 9th stage of the pushover analysis. The 9th stage simulates most of the internal joint shear failures and the formation of plastic hinges on the internal and external beams throughout the structure. Furthermore, the results reveal that the soft story mechanism began to emerge on the fifth-floor level but did not fully appear until the tenth step, which was mainly due to the reduced longitudinal steel amount in the columns from the 5th floor onwards. When Stage 9 is compared to the degree of damage to the real structure, a significant correlation is revealed.

4.1.1 The Capacity Spectrum Method and Resulting ADRS

The Capacity Spectrum Method is utilized for the performance-based non-linear analysis of this structure. The resulting ADRS (Acceleration Displacement Response Spectra) plot is shown in Figure 4.3. As noted in the methodology section, converting both curves to ADRS format facilitates plotting the demand and capacity curves on a single graph, under the domain of spectral acceleration and spectral displacement, allowing for identifying the building's approximate displacement during the earthquake by locating the curves' intersection points. As a result of the capacity spectrum method, the approximate displacement is expected to range between 37 and 117 mm, which results in the deflection profile shown at stage 9 of the pushover analysis. It should be noted that in the ADRS approach, only the horizontal earthquake motions can be considered. However, as stated before, the vertical accelerations can cause variations in column axial forces that can affect the behavior

of the RC beam-column joints. To investigate this aspect further, more advanced time history analyses incorporating vertical acceleration effects are performed. The results of these analyses are reported in the next section.

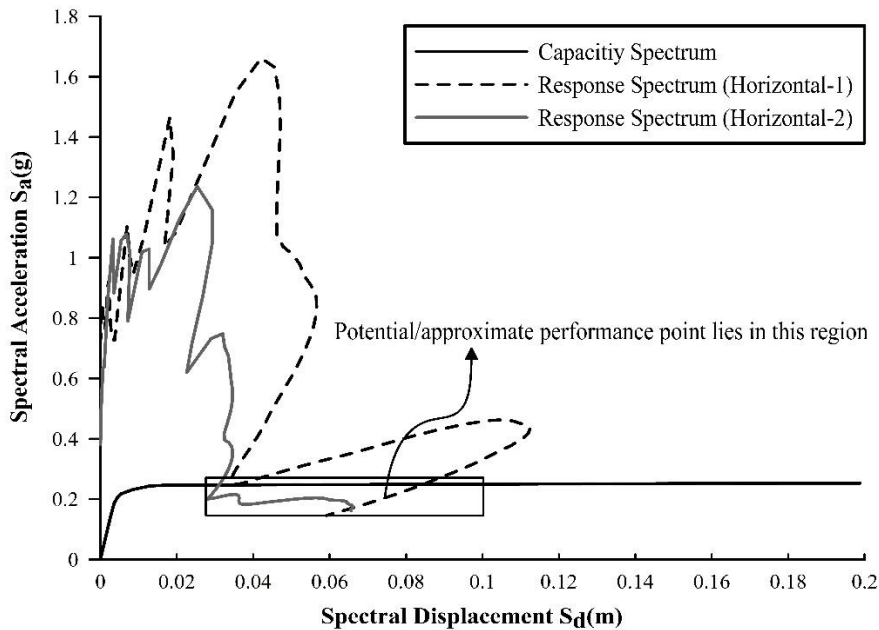


Figure 4.3. Acceleration Displacement Response Spectra (ADRS)

4.2 Time-History Analysis Results

The earthquake data mentioned in the methodology section are used to conduct time-history analyses. Two independent analyses are carried out with three distinct data sets, two corresponding to horizontal seismic motions and one to vertical acceleration. Given that the study is conducted on a two-dimensional plane with only one frame of the building chosen, the predominant response direction of the structure is difficult to simulate. Therefore, both horizontal acceleration recordings are used in the time-history analyses carried out, and the true response is expected to be

somewhat in between both analyses. The next subsections show the results for the analyses carried out with/without the vertical accelerations.

4.2.1 Horizontal-1 Only and Horizontal-1 with Vertical Acceleration

The time history results reported in this section contain the analysis results obtained using the Horizontal-1 only and the Horizontal-1 with simultaneous vertical acceleration ground motion data (shown in Figure 4.4). Since the time history functions contain 110 seconds of earthquake ground motion data with a 0.05-second increment, out of 22000 solution steps, only a few steps simulating failure patterns are selected and shown for each analysis.

Comparing analyses with and without the vertical seismic motion, different failures occurring throughout the frame are circled to facilitate their visibility in Figure 4.4. At 8.48 seconds in Figure 4.4, joint failures in the internal joints of the second, fourth and fifth-floor levels are observed when vertical acceleration is included, whereas those joint failures could not be observed with only the horizontal ground motion. It is important to note that, whether with or without vertical acceleration, plastic hinges formed prior to joint failures on the second floor, whereas joint failures on the other floors happened prior to the formation of plastic hinges on the beams. As it can be seen by the results at 9.635 seconds, while the internal beam-column joints fail in the analysis with the vertical acceleration, the same failures cannot be observed in the analysis without the vertical acceleration.

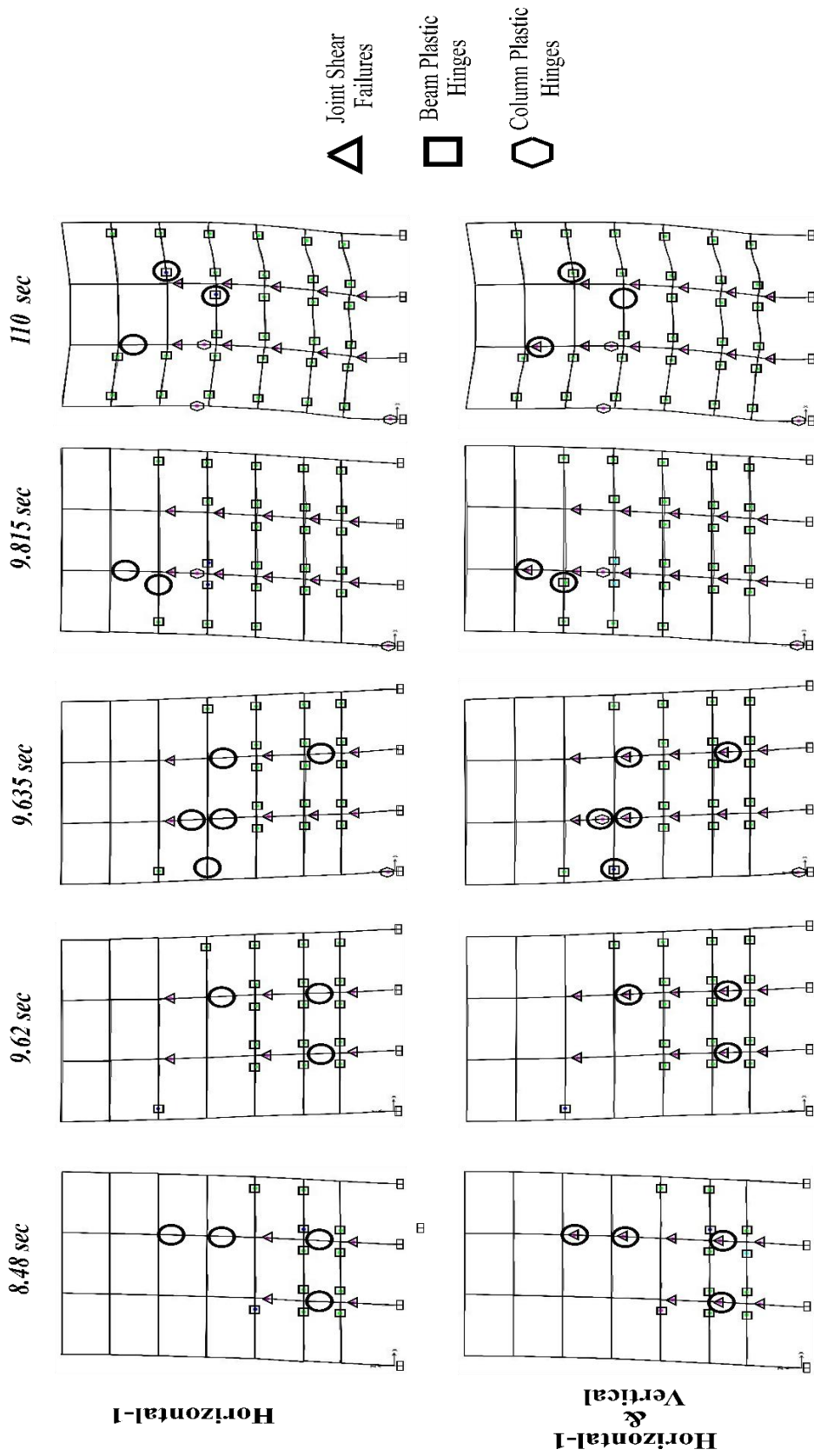


Figure 4.4. Results of time history analysis with only horizontal-1 and horizontal-1 with vertical acceleration (8.4 sec; 9.62 sec; 9.635 sec; 9.815 sec; 110 sec)

According to the analysis carried out, it can be stated that the model is simple yet effective in representing the potential failures expected to occur at the internal and/or external beam-column joints. Among these analyses, the sequence of failures expected at the RC beam-column joint seems to differ based on whether vertical accelerations are considered or not. The final state of the expected damage in the structure at the Ultimate Limit State (ULS) does not look very different in both analyses carried out (without/with vertical accelerations): only minor variances such as plastic hinge formations on internal beam ends and internal joint failure on the sixth level can be observed at the ULS of the structure. As noted in the pushover analysis results, the soft story mechanism is not triggered fully in building. Therefore, it can be inferred that the presence of vertical accelerations can facilitate the earlier formation of some damage types normally expected at later drift levels in the structure.

4.2.2 Horizontal-2 Only and Horizontal-2 with Vertical Acceleration

Similar to the previous analysis results, only a few analysis steps are shown in Figure 4.5: three stages corresponding to 8.485 seconds, 8.975 seconds, and 110 seconds for analyses with and without vertical acceleration.

Analyses conducted with the horizontal and vertical earthquake ground motion data reveal two differences in the first stage, corresponding to the 8.485 seconds of the time history. At this stage, except for the internal joint on the fifth story, the majority of internal joint failures from the first to fifth floors are seen prior to beam plastic

hinge formation in both investigations. Additionally, no plastic hinge forms on external joints subjected to only horizontal acceleration. It should be noted that study results are obtained for each 0.05-second time frame using 22000 earthquake data for each direction. The structure's response is generally the same in this analysis regardless of the vertical acceleration employed. As a result, only three stages are displayed in Figure 4.5. In the second stage, which takes 8.975 seconds, both analyses show the failure of all internal joints up to the fifth floor. All of the time history analyses are completed at the 110-second mark, depicted as the final step in Figure 4.5. The failure results in the structure are identical to those caused by the vertical acceleration effect.

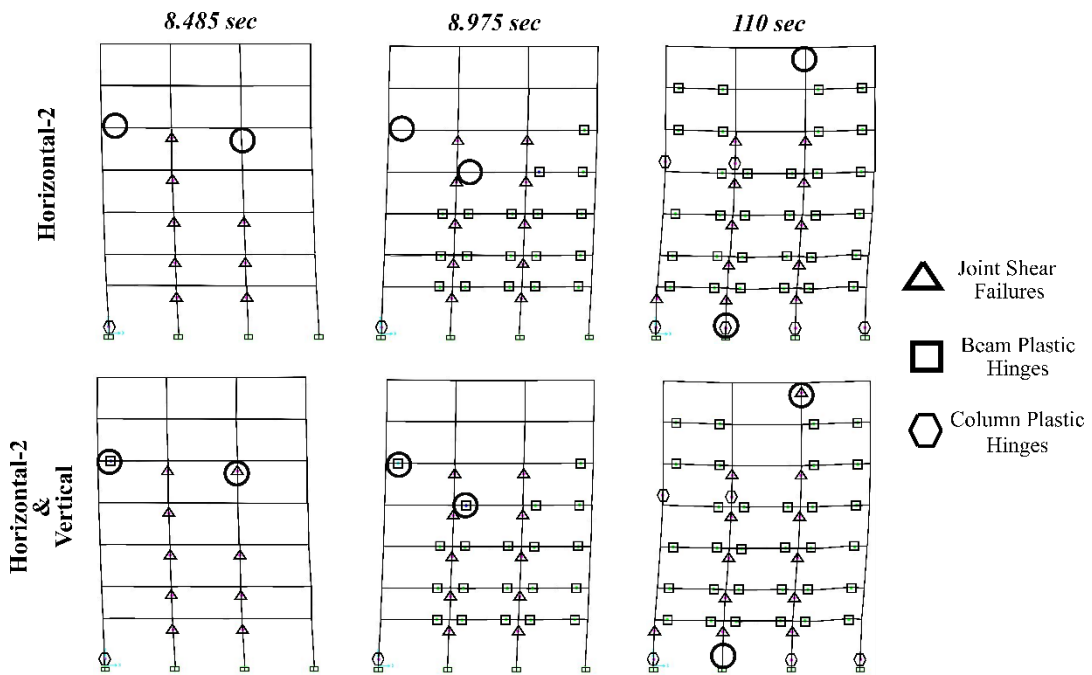


Figure 4.5. Results of time history analysis with Horizontal-2 and Vertical data (8.485 sec; 8.975 sec; 110 sec)

4.3 Discussion of Results

The pushover analysis results by employing the novel RC beam-column joint model show a behavior remarkably similar to the observations on the structure following the considered earthquake. In this study, pushover analysis mainly reveals the potential joint shear failures expected at the internal beam-column joints and the expected plastic hinge formations to occur at the connected beams (mostly after the formation of the joint shear failures). However, these plastic hinges are questionable in reality since the joint shear damage precedes the beam plastic hinge formation. Therefore, the internal beam-column joint shear damage is expected to worsen rather than forming a plastic hinge at the connected beam, which is in agreement with the observed damage.

Overall, the pushover analysis shows that the used novel RC beam-column joint model can accurately describe the response of the structure accurately when used in non-linear static analysis. Additionally, due to the absence of a soft-story failure on the fifth floor in the real structure, likely, the structure was not pushed to this level during the earthquake. It should be noted that beginning on the fifth floor, the column reinforcing was reduced, potentially causing the soft story observed in the pushover analysis' later stages.

In addition to the pushover analysis, four main time history analyses are performed: two for two distinct horizontal data sets (Horizontal-1, Horizontal-2) and two for simulating the vertical acceleration effects. Although the findings for Horizontal-1 show the internal beam-column joint failures, plastic hinge formation occurs prior to

joint failures in some floor beams, which is the expected behavior in modern buildings (i.e., beam sway mechanism). However, this behavior does not reflect the actual response of the building since no plastic hinges were observed at the beams connected to the internal RC beam-column joints after the earthquake. Compared to the Horizontal-1 data, analyses using the Horizontal-2 ground motion data reveal few differences when vertical acceleration is considered. The results indicate that the vertical acceleration effect is not as large as in the initial Horizontal-1 investigation. However, it more properly depicts/simulates the case study building's behavior. All internal joints fail prior to the beam plastic hinges in this analysis, contrary to the expectations of the capacity design.

When the pushover and time history analysis results are compared to the observations on structure after the 22 February 2011 Christchurch earthquake, it becomes apparent that the previously proposed beam-column joint model can accurately simulate the building response. Additionally, completing time history analyses with vertical acceleration illustrates the model's efficacy in predicting joint behavior under varying axial loads, as evidenced by both analyses utilizing horizontal-1 and horizontal-2 earthquake data. However, the vertical accelerations currently seem to affect the sequence of failures expected within the structure, while the expected damage at ULS seems similar for both analysis types (non-linear static and time history analyses).

CHAPTER 5

CONCLUSIONS

The article describes implementing a novel RC beam-column joint model in the widely used structural analysis software SAP2000. The model depicts joint shear capacity as an N-M interaction envelope and is aimed for use by practical engineers in real engineering applications. Modeling the beam-column joint as an N-M interaction would be particularly useful for incorporating the axial load level change into the capacity representation of beam-column joints. This cannot be accounted for moment-rotation relationship models because moment-rotation responses are obtained using a constant or specific axial load value; therefore, it would be impractical to account for variations in axial load because the moment-rotation relationship would vary with each axial load level. Defining a plastic hinge with the moment-rotation relationship for a beam-column joint may be difficult due to the presence of unknowns. For instance, one must assume a particular axial load value on the corresponding joint to define moment-rotation. On the other hand, the simplified N-M interaction consists of only three points that can be calculated using a straightforward method, and engineers do not have to deal with unknowns such as the specific axial load assumption. In addition, the model can be easily implemented in structural analysis software using plastic hinges defined by N-M interaction, similar to a column N-M interaction chart. The model is validated by examining a

case study building in Christchurch, New Zealand, struck by an earthquake on February 22, 2011. The building is a rarely encountered example of the observed failure pattern. Although it was constructed to meet capacity design specifications and incorporate sufficient joint shear reinforcement, it suffered joint shear damage. The joint model used in this study can simultaneously simulate two types of joint shear mechanisms: i) principal tension dominated joint shear mechanism; and ii) principal compression dominated joint shear mechanism. As a result, it is possible to account for capacity changes induced by varying axial load levels that are expected to vary during any seismic action.

The N-M interaction model is illustrated utilizing non-linear static (pushover) and non-linear dynamic (time history) analyses on a two-dimensional non-linear model. The results are compared to the real damage observation data acquired following the earthquake. The front frame of the building is selected since it exhibits joint shear damage evidently. The analysis results demonstrate a significant correlation with damage observations, and the model accurately simulates joint shear response.

In order to illustrate the practicality of the model and any potential behavioral changes caused by the vertical accelerations during the earthquake, the vertical accelerations are simultaneously applied to the structure alongside the horizontal accelerations in the time history analyses. Time history analyses are carried out first without the vertical accelerations and then with the vertical accelerations. The results of these two analyses did not differ significantly from each other, considering their

ULS (final damaged state). However, the vertical accelerations are found to affect the sequence of the failures expected within the structure during an earthquake.

It can be concluded that the model used in this article can practically be utilized in both non-linear static and non-linear dynamic time history analyses: the final damaged state of the structure did not differ significantly between these analysis types. The model is able to simulate the beam-column joint response with relatively high accuracy compared to the damage observations of the example building. More experimental research is needed to show the effects of the high/extreme axial loads on the behavior of the RC beam-column joints.

5.1 Sustainability

The construction industry is one of the most significant contributors to the three components of sustainability (e.g., environmental, economic, and social). A building's earthquake resistance and performance during an earthquake are directly related to its sustainability, as any structure with poor seismic performance may result in its destruction, collapse, or need for repair. Although the direct effect of seismic performance/damage can be estimated using life cycle assessment procedures, this study does not include such analysis due to a lack of information on the case study structure. However, several case studies are shown in the literature section that performs life cycle analysis on RC buildings incorporating seismic performance to determine their impact on sustainability. According to the findings of these studies and other information in the literature, a structure's performance

during an earthquake can significantly impact the environment, economy, and society.

Moreover, in this study, a simplified N-M interaction beam-column joint model is implemented into the analysis software that can be used to evaluate the building's performance and can represent the beam-column joint capacity under various axial load levels. This research aims to achieve a more precise evaluation of seismic performance, which is directly related to sustainability, by simulating the response of beam-column joints more accurately with the incorporation of axial load variation. Compared to the actual damage observations of the example building, the results show that the model can simulate the beam-column joint response with a relatively high degree of accuracy, resulting in a more precise evaluation of seismic performance.

5.2 Limitations

It should be noted that this work is carried out on a 2D seismic frame taken from a real structure that experienced the February 2011 Christchurch Earthquake in New Zealand. Since the study is only based on a 2D frame, certain effects have not been considered. Those effects are bi-directional loading, floor torsion, P-delta, and the interaction among the frames in the perpendicular directions. However, the reported analyses showed to be accurate enough to approximately identify the damage patterns suffered by this particular building during the earthquake

REFERENCES

- Anwar, G.A. Dong, Y. and Zhai, C. [2019] "Performance-based probabilistic framework for seismic risk, resilience, and sustainability assessment of reinforced concrete structures," *Advances in Structural Engineering* 23 (7), 1454-1472. 10.1177/1369433219895363.
- Arukala, S.R. Pancharathi, R.K. and Pulukuri, A.R. [2019] "Evaluation of sustainable performance indicators for the built environment using ahp approach," *Journal of The Institution of Engineers (India): Series A* 100 (4), 619-631. 10.1007/s40030-019-00405-8.
- ATC-40. 1996. Seismic evaluation and retrofit of concrete buildings. Commission, S.S., California, U.S.A.
- Beckingsale, C.W., 1980. Post elastic behaviour of reinforced concrete beam-column joints. PhD Thesis, University of Canterbury.
- Bird, J.F. and Bommer, J.J. [2004] "Earthquake losses due to ground failure," *Engineering Geology* 75 (2), 147-179. 10.1016/j.enggeo.2004.05.006.
- Birely, A.C. Lowes, L.N. and Lehman, D.E. [2012] "A model for the practical non-linear analysis of reinforced-concrete frames including joint flexibility," *Engineering Structures* 34, 455-465. 10.1016/j.engstruct.2011.09.003.
- Borghini, A. Gusella, F. and Vignoli, A. [2016] "Seismic vulnerability of existing r.C. Buildings: A simplified numerical model to analyse the influence of the beam-column joints collapse," *Engineering Structures* 121, 19-29. 10.1016/j.engstruct.2016.04.045.
- Bradley, B.A. and Cubrinovski, M. [2011] "Near-source strong ground motions observed in the 22 february 2011 christchurch earthquake," *Seismological Research Letters* 82 (6), 853-865. 10.1785/gssrl.82.6.853.
- Chhabra, J.P.S. Hasik, V. Bilec, M.M. and Warn, G.P. [2018] "Probabilistic assessment of the life-cycle environmental performance and functional life of buildings due to seismic events," *Journal of Architectural Engineering* 24 (1). 10.1061/(asce)ae.1943-5568.0000284.

- Comber, M.V. Poland, C. and Sinclair, M. [2012] Environmental impact seismic assessment: Application of performance-based earthquake engineering methodologies to optimize environmental performance, Structures Congress 2012. Structures Congress, Chicago, Illinois, United States.
- Çavdar, Ö. and Bayraktar, A. [2013] "Pushover and non-linear time history analysis evaluation of a rc building collapsed during the van (turkey) earthquake on october 23, 2011," *Natural Hazards* 70 (1), 657-673. 10.1007/s11069-013-0835-3.
- Elmorsi, M. Kianoush, M.R. and Tso, W.K. [2000] "Modeling bond-slip deformations in reinforced concrete beam-column joints," *Canadian Journal of Civil Engineering* 27, 490-505.
- Ersoy, U. Özcebe, G. and Tankut, T. [2003] Reinforced concrete, METU PRESS, Ankara, TR.
- Fardis, M.N. [2018] "Capacity design: Early history," *Earthquake Engineering & Structural Dynamics* 47 (14), 2887-2896. 10.1002/eqe.3110.
- Favvata, M.J. Izzuddin, B.A. and Karayannis, C.G. [2008] "Modelling exterior beam-column joints for seismic analysis of rc frame structures," *Earthquake Engineering & Structural Dynamics* 37 (13), 1527-1548. 10.1002/eqe.826.
- FEMA. 2018. Seismic performance assessment of buildings-methodology. Washington, DC
- FEMA. 2018. Seismic performance assessment of buildings-methodology for assessing environmental impacts. Washington, DC
- French, S.P. [2018] Connecting physical damage to social and economic impacts, 17th U.S.-Japan-New Zealand Workshop on the Improvement of Structural Engineering and Resilience. Queenstown, New Zealand.
- Gencturk, B. and Hossain, K. [2013] Structural performance assessment in the context of seismic sustainability, International Concrete Sustainability Conference. San Francisco, CA.
- Gencturk, B. Hossain, K. and Lahourpour, S. [2016] "Life cycle sustainability assessment of rc buildings in seismic regions," *Engineering Structures* 110, 347-362. 10.1016/j.engstruct.2015.11.037.

- Gordon, P. Moore, J.E. Richardson, H.W. Shinozuka, M. An, D. and Cho, S. [2004] "Earthquake disaster mitigation for urban transportation systems: An integrated methodology that builds on the kobe and northridge experiences," *Modeling spatial and economic impacts of disasters*. Springer Berlin Heidelberg, In Okuyama, Y. and Chang, S.E. (eds), Berlin, Heidelberg, pp. 205-232.
- Hossain, K.A. and Gencturk, B. [2014] "Life-cycle environmental impact assessment of reinforced concrete buildings subjected to natural hazards," *Journal of Architectural Engineering* 22 (4). 10.1061/(ASCE).
- Irfani, M.M.A. and Vimala, A. [2019] "Collapse mechanism of strong column weak beam buildings of varying heights," *International Journal of Engineering and Advanced Technology* 9 (1), 4144-4148. 10.35940/ijeat.A1380.109119.
- Kalantari, A. [2012] *Seismic risk of structures and the economic issues of earthquakes*, Earthquake engineering In Sezen, H. (ed), London.
- Kazimi, A.A. and Mackenzie, C.A. [2016] *The economic costs of natural disasters, terroris attacks, and other calamities: An analysis of economic models that quantify the losses caused by disruptions*, IEEE Systems and Information Engineering Design Symposium (SIEDS). pp. 32-37.
- Khan, M.A. [2013] *Seismic design for buildings, Earthquake-resistant structures*.
- Kim, J. and LaFave, J.M. [2007] "Key influence parameters for the joint shear behaviour of reinforced concrete (rc) beam–column connections," *Engineering Structures* 29 (10), 2523-2539. 10.1016/j.engstruct.2006.12.012.
- Lima, L. Trindade, E. Alencar, L. Alencar, M. and Silva, L. [2021] "Sustainability in the construction industry: A systematic review of the literature," *Journal of Cleaner Production* 289, 125730. 10.1016/j.jclepro.2020.125730.
- Masi, A. Santarsiero, G. Lignola, G.P. and Verderame, G.M. [2013] "Study of the seismic behavior of external rc beam–column joints through experimental tests and numerical simulations," *Engineering Structures* 52, 207-219. 10.1016/j.engstruct.2013.02.023.
- May, P.J. [2001] "Societal perspectives about earthquake performance: The fallacy of 'acceptable risk'," *Earthquake Spectra* 17 (4), 725-737. 10.1193/1.1423904].

- May, P.J. 2007. Societal implications of performance-based earthquake engineering. University of Washington
- Menna, C. Asprone, D. Jalayer, F. Prota, A. and Manfredi, G. [2012] "Assessment of ecological sustainability of a building subjected to potential seismic events during its lifetime," *The International Journal of Life Cycle Assessment* 18 (2), 504-515. 10.1007/s11367-012-0477-9.
- Negro, P. [2014] Seismic performance assessment addressing sustainability and energy efficiency
- NRC [1992] The economic consequences of a catastrophic earthquake: Proceedings of a forum, The National Academies Press, Washington, DC.
- Pan, Z. Guner, S. and Vecchio, F.J. [2017] "Modeling of interior beam-column joints for non-linear analysis of reinforced concrete frames," *Engineering Structures* 142, 182-191. 10.1016/j.engstruct.2017.03.066.
- Park, R. and Paulay, T. [1975] Reinforced concrete structures, Jhon Wiley & Sons, New York.
- Park, R. and Ruitong, D. [1988] "A comparison of the behaviour of reinforced concrete beam-column joints designed for ductility and limited ductility," *Bulletin of the New Zealand National Society for Earthquake Engineering* 21 (4), 255-278.
- Parker, M. and Steenkamp, D. [2012] "The economic impact of the canterbury earthquakes," *Reserve Bank of New Zealand Bulletin* 75.
- Patil, A.S. and Kumbhar, P.D. [2013] "Time history analysis of multistoried rcc buildings for different seismic intensities," *International Journal of Structural and Civil Engineering Research* 2.
- Paulay, T. and Scarpas, A. [1981] "The behaviour of exterior beam-column joints," *Bulletin of the New Zealand National Society for Earthquake Engineering* 14 (3), 131-144.
- Presley, A. Sarkis, J. and Meade, L. [2010] "Benchmarking for sustainability: An application to the sustainable construction industry," *Benchmarking: An International Journal* 17 (3), 435-451. 10.1108/14635771011049380.

- Ricci, P. De Luca, F. and Verderame, G.M. [2010] "6th april 2009 l'aquila earthquake, italy: Reinforced concrete building performance," *Bulletin of Earthquake Engineering* 9 (1), 285-305. 10.1007/s10518-010-9204-8.
- Sarkisian, M.P. [2013] "Design of environmentally responsible structures in regions of high seismic risk," *Structure and Infrastructure Engineering* 10 (7), 849-864. 10.1080/15732479.2012.761249.
- Sezen, H. Whittaker, A.S. Elwood, K.J. and Mosalam, K.M. [2003] "Performance of reinforced concrete buildings during the august 17,1999 kocaeli,turkey earthquake, and seismic desing and construction practise in turkey," *Engineering Structures* 25, 103-114.
- Shafaei, J. Zareian, M.S. Hosseini, A. and Marefat, M.S. [2014] "Effects of joint flexibility on lateral response of reinforced concrete frames," *Engineering Structures* 81, 412-431. 10.1016/j.engstruct.2014.09.046.
- Tae, S. Baek, C. and Shin, S. [2011] "Life cycle co2 evaluation on reinforced concrete structures with high-strength concrete," *Environmental Impact Assessment Review* 31 (3), 253-260. 10.1016/j.eiar.2010.07.002.
- Tanner, A. Chang, S.E. and Elwood, K.J. [2020] "Incorporating societal expectations into seismic performance objectives in building codes," *Earthquake Spectra* 36 (4), 2165-2176. 10.1177/8755293020919417.
- Tasligedik, A.S. [2022] "Shear capacity n-m interaction envelope for rc beam-column joints with transverse reinforcement: A concept derived from strength hierarchy," *Journal of Earthquake Engineering*, 1-31. 10.1080/13632469.2020.1756988.
- Tasligedik, A.S. Akguzel, U. Kam, W.Y. and Pampanin, S. [2018] "Strength hierarchy at reinforced concrete beam-column joints and global capacity," *Journal of Earthquake Engineering* 22 (3), 454-487. 10.1080/13632469.2016.1233916.
- Unal, M. and Burak, B. [2013] "Development and analytical verification of an inelastic reinforced concrete joint model," *Engineering Structures* 52, 284-294. 10.1016/j.engstruct.2013.02.032.
- Wei, H.-H. Shohet, I.M. Skibniewski, M.J. Shapira, S. and Yao, X. [2016] "Assessing the lifecycle sustainability costs and benefits of seismic mitigation designs for buildings," *Journal of Architectural Engineering* 22 (1). 10.1061/(asce)ae.1943-5568.0000188.

Wei, H.-H. Skibniewski, M.J. Shohet, I.M. and Yao, X. [2016] "Lifecycle environmental performance of natural-hazard mitigation for buildings," *Journal of Performance of Constructed Facilities* 30 (3).
10.1061/(asce)cf.1943-5509.0000803.

Youssef, M. and Ghobarah, A. [2008] "Modelling of rc beam-column joints and structural walls," *Journal of Earthquake Engineering* 5 (1), 93-111.
10.1080/13632460109350387.

APPENDICES

A. Shear Capacity Envelopes

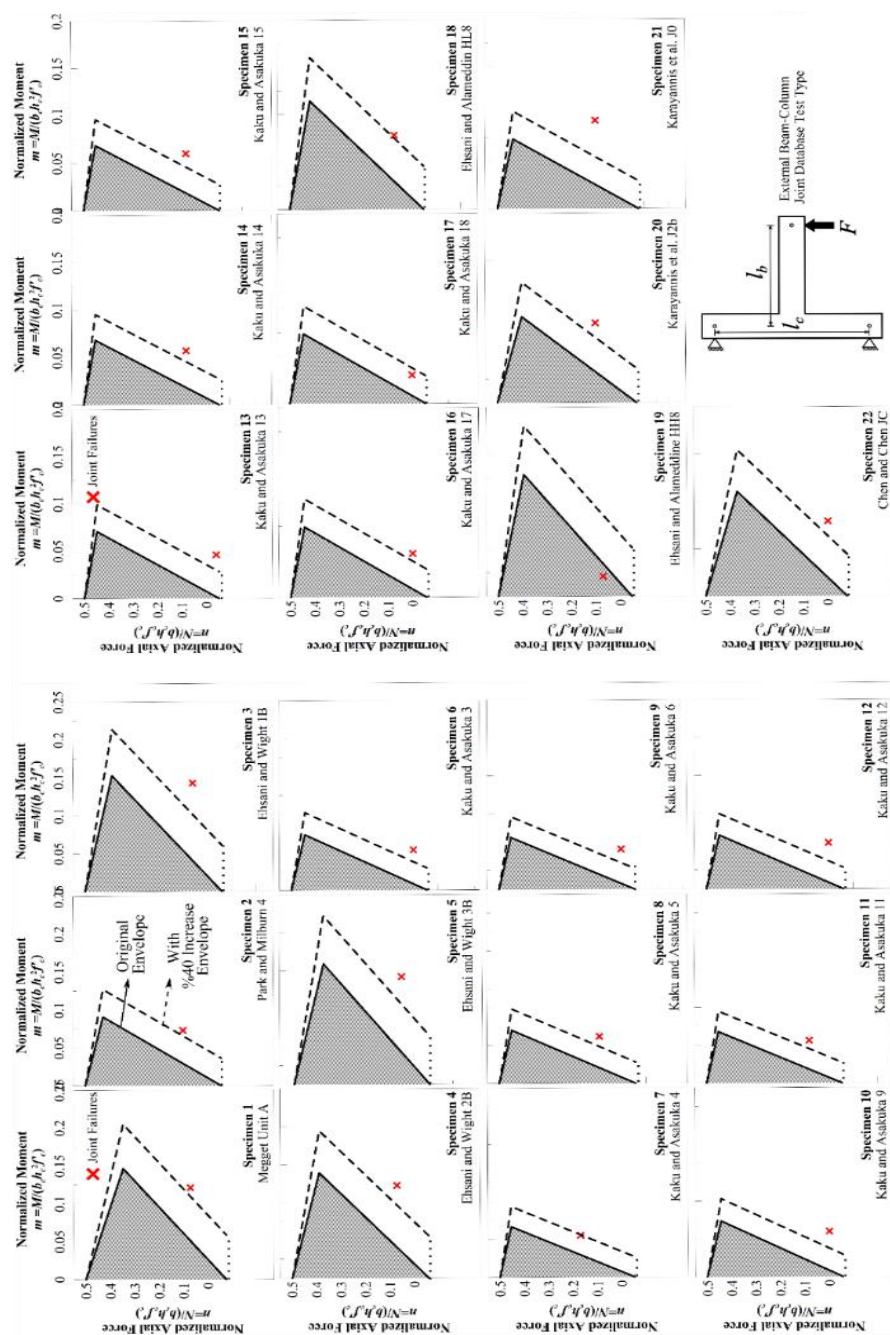


Figure 5.1. Normalized joint N-M interaction envelopes with the 40% increase (dashed) and the original envelopes (grey envelope) for 22 external beam-column joints (Tasligedik 2020)

TEZ İZİN FORMU / THESIS PERMISSION FORM

PROGRAM / PROGRAM

Sürdürülebilir Çevre ve Enerji Sistemleri / Sustainable Environment and Energy Systems

Siyaset Bilimi ve Uluslararası İlişkiler / Political Science and International Relations

İngilizce Öğretmenliği / English Language Teaching

Elektrik Elektronik Mühendisliği / Electrical and Electronics Engineering

Bilgisayar Mühendisliği / Computer Engineering

Makina Mühendisliği / Mechanical Engineering

YAZARIN / AUTHOR

Soyadı / Surname : Sahutoglu

Adı / Name : Orhan

Programı / Program : Sustainable Environment and Energy Systems

TEZİN ADI / TITLE OF THE THESIS (İngilizce / English) :
Understanding the Behaviour of Modern Reinforced Concrete
Beam-Column Joints towards
the Development of a Simplified Structural Model

TEZİN TÜRÜ / DEGREE: Yüksek Lisans / Master Doktora / PhD

1. Tezin tamamı dünya çapında erişime açılacaktır. / Release the entire work immediately for access worldwide.

2. Tez iki yıl süreyle erişime kapalı olacaktır. / Secure the entire work for patent and/or proprietary purposes for a period of two years. *

3. Tez altı ay süreyle erişime kapalı olacaktır. / Secure the entire work for period of six months. *

Yazarın imzası / Author Signature **Tarih / Date**

Tez Danışmanı / Thesis Advisor Full Name:

Tez Danışmanı İmzası / Thesis Advisor Signature:

Eş Danışmanı / Co-Advisor Full Name:

Eş Danışmanı İmzası / Co-Advisor Signature:

Program Koordinatörü / Program Coordinator Full Name:

Program Koordinatörü İmzası / Program Coordinator Signature: